

MULTIRATE SYSTEMS AND FILTER BANKS

Tapio Saramäki and Robert Bregović
Signal Processing Laboratory, Tampere University of Technology
P.O. Box 553, FIN-33101 Tampere, Finland

1 Introduction

During the last two decades, multirate filter banks have found various applications in many different areas, such as speech coding, scrambling, adaptive signal processing, image compression, signal and image processing applications as well as transmission of several signals through the same channel (Malvar, 1992a; Vaidyanathan, 1993; Vetterli and Kovačević, 1995; Fliege, 1994; Misiti, Misiti, Oppenheim, and Poggi, 1996). The main idea of using multirate filter banks is the ability of the system to separate in the frequency domain the signal under consideration into two or more signals or to compose two or more different signals into a single signal.

When splitting the signal into two or more signals an analysis-synthesis system is used. The analysis-synthesis systems under consideration in this chapter are critically sampled multi-channel or M -channel uniform filter banks and octave filter banks as shown in Figures 1(a) and 1(b), respectively. In the analysis bank of the uniform bank, the signal is split with the aid of M filters $H_k(z)$ for $k=0,1,\dots,M-1$ into M bands of the same bandwidth and each sub-signal is decimated by a factor of M . In the case of octave filter banks, the overall signal is first split into two bands of the same bandwidth and both sub-signals are decimated by a factor of two. After that, the decimated lowpass filtered signal is split into two bands and so on. Doing this three times gives rise to a three-level octave filter bank corresponding to the structure shown in Figure 1(b). In this case, $H_0(z)$ is a highpass filter with bandwidth equal to half the baseband and the decimation factor is 2, $H_1(z)$ and $H_2(z)$ are bandpass filters with bandwidths equal to one fourth and one eighth of the baseband, respectively, and the corresponding decimation factors are 4 and 8, whereas $H_3(z)$ is a lowpass filter with the same bandwidth and decimation factor as $H_2(z)$.

In many applications, the processing unit corresponds to storing the signal into the memory or transferring it through the channel. The main goal is to significantly reduce, with the aid of proper coding schemes, the number of bits representing the original signal for storing or transferring purposes. When splitting the signal into various frequency bands with the aid of the analysis filter bank, the signal characteristics are different in each band and various numbers of bits can be used for coding and decoding the sub-signals. In some applications, the processing unit is used for treating the sub-signal in order to obtain the desired operation for the output signal of the overall system. A typical example is the use of the overall system for making adaptive signal processing more efficient. Another example is the de-noising of a signal performed with the aid of a special octave filter bank, called a discrete-time wavelet bank (Vetterli and Kovačević, 1995; Misiti et al., 1996).

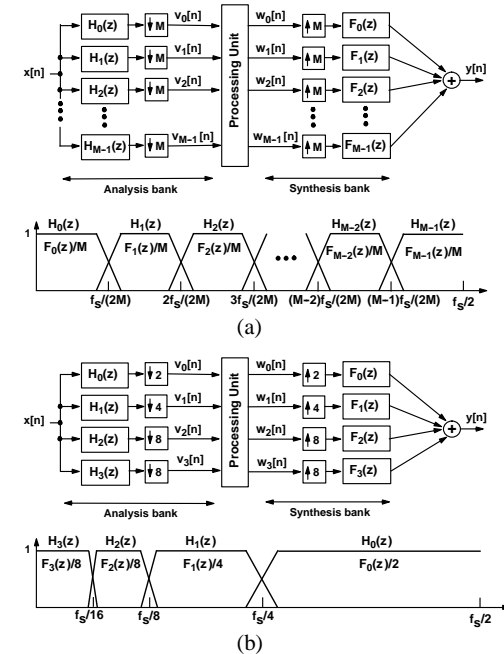


Figure 1. Analysis-synthesis filter bank. (a) M -channel uniform filter bank. (b) Three-level octave filter bank. Note that in the case of interpolation by a given factor, the corresponding filter should approximate this factor in the passband in order to preserve the signal energy.

The role of the filters in the synthesis part is to approximately reconstruct the original signal. This is performed in two steps. First, for the uniform filter bank, the M sub-signals at the output of the processing unit are interpolated by a factor of M and filtered by M synthesis filters $F_k(z)$ for $k=0,1,\dots,M-1$, whereas for the octave filter bank, the interpolation factors for the sub-signals are the same as for the analysis part. Second, the outputs of these filters are added. In the transferring and storing applications, the ultimate goal is to design the overall system such that, despite of a significantly reduced number of bits used in the processing unit, the reconstructed signal is either a delayed version of the original signal or suffers from a negligible loss of information carried by the sub-signals.

There are two types of coding techniques, namely, lossy and lossless codings. For the lossless coding, it is desired to design the overall system such that the output signal is simply a delayed version of the input signal or suffers from some phase distortion being tolerable in some applications. For the lossy coding, it is beneficial to design the analysis-synthesis filter bank such that some distortions, including amplitude distortion and aliasing errors, being less than those caused by coding distortions are allowed. This increases the overall filter bank performance or, alternatively, the same performance can be achieved by shorter filter orders or a shorter delay caused for the input signal by the overall filter bank. These facts are very crucial for speech,

audio, and communication applications. The coding techniques are not considered at all in this chapter and we concentrate on the case where the processing unit does not cause any errors to the sub-signals.

In the case of audio or speech signals, the goal is to design the overall system together with coding such that our ears are not able to notice the errors caused by reducing the number of bits used for storing or transferring purposes. In the case of images our eyes serve as "referees", that is, the purpose is to reduce the number of bits to represent the image to the limit that is still satisfactory to our eyes.

Depending on how many channels are used for the signal separation, there are two groups of uniform filter banks, namely, multi-channel or M -channel filter banks ($M > 2$) and two-channel filter banks ($M = 2$). In the first group, the signal is separated into M different channels and in the second group into two channels. Using a tree-structure, two-channel filter banks can be used for building M -channel filter banks in the case where M is a power of two. A more effective way of building M -channel filter banks is to first design a prototype filter in a proper manner. The filters in the analysis and synthesis banks are then generated with the aid of this prototype filter by using a cosine-modulation or a modified discrete Fourier transform (MDFT) technique (Malvar, 1992b; Vaidyanathan, 1993; Fliege, 1993; Heller, Karp, and Nguyen 1999; Karp, Mertins, and Schuller 2001).

Two-channel filter banks are very useful in generating octave filter banks. In this case, the overall signal is first split with the aid of a two-channel filter bank into two bands. After that, the decimated lowpass filtered signal is split into two bands using the same two-channel filter bank and so on. There are two basic types of octave filter banks, namely, frequency-selective filter banks mostly used for audio and telecommunications applications and discrete-time wavelet banks used in applications where the signal waveform is desired to be preserved, like in the case of images. For discrete-time wavelet banks, the frequency selectivity of the filters in the octave analysis-synthesis filter banks is not so important due to their different applications. There are other properties that are more important, as will be discussed in Subsection 4.2 and in more details in Chapter 3. In these cases, the main goal is to preserve the waveform of the input signal after treating it in an appropriate manner in the processing unit.

When two or more different signals are composed into a single signal, then a uniform synthesis-analysis system is used, as shown in Figure 2. This system is also called a transmultiplexer. In this system, all the M signals are interpolated by a factor of M and filtered by M synthesis filters $F_k(z)$ for $k = 0, 1, \dots, M-1$. Then, the outputs are added to give a single signal with sampling rate being M times that of the input signals. The next step is to transfer the signal through a channel. Finally, in the analysis bank the original signals are reconstructed with the aid of M analysis filters $H_k(z)$ for $k = 0, 1, \dots, M-1$. These signals have the original sampling rates due to the decimation by a factor of M . If the output signal in the analysis-synthesis system is just a delayed version of the input signal, then for the corresponding transmultiplexer the output signals in the case of the ideal channel are delayed versions of the inputs. Therefore, the design of a transmultiplexer can be converted to the design of an analysis-synthesis filter bank. Based on this fact, this chapter does not consider the design of transmultiplexers. An interested reader is referred to the textbook written by Fliege (1993).

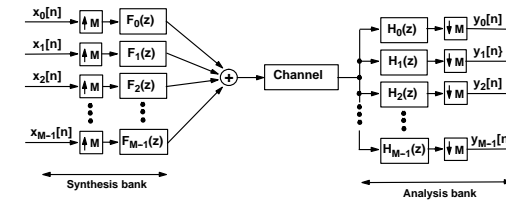


Figure 2. Synthesis-analysis filter bank: Transmultiplexer.

The outline of this chapter is as follows. Section 2 reviews various types of existing finite impulse response (FIR) and infinite impulse response (IIR) two-channel filter banks. The basic operations of these filter banks are considered and the requirements are stated for alias-free, perfect-reconstruction (PR), and nearly perfect-reconstruction (NPR) filter banks. Also some efficient synthesis techniques are referred to. Furthermore, examples are included to compare various two-channel filter banks with each other. Section 3 concentrates on the design of multi-channel (M -channel) uniform filter banks. The main emphasis is laid on designing these banks using tree-structured filter banks with the aid of two-channel filter banks and on generating the overall bank with the aid of a single prototype filter and a proper cosine-modulation or MDFT technique. In Section 4, it is shown how octave filter banks can be generated using a single two-channel filter bank as the basic building block. Also, the relations between the frequency-selective octave filter banks and discrete-time wavelet banks are briefly discussed. Finally, concluding remarks are given in Section 5.

2 Two-Channel Filter Banks

This section considers the synthesis of two-channel filter banks based on the use of FIR and IIR filters. First, basic operation principles are discussed and the necessary requirements for alias-free, perfect-reconstruction (PR), and nearly PR (NPR) filter banks are stated. Second, an overview of the most important filter bank types and references to some existing synthesis schemes are given.

2.1 Basic Operation of a Two-Channel Filter Bank

The block diagram of a two-channel filter bank is shown in Figure 3. This system consists of an analysis and a synthesis bank as well as a processing unit between these two banks.

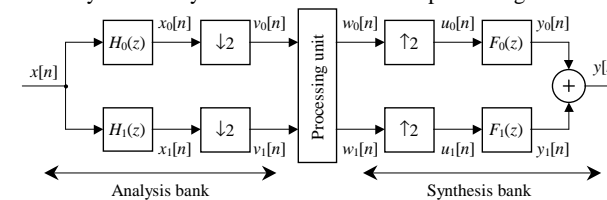


Figure 3. Two-channel filter bank.

2.1.1 Operation of the analysis bank

The role of the analysis bank is to split the input signal $x[n]$ into lowpass and highpass filtered channel signals, denoted by $x_0[n]$ and $x_1[n]$ in Figure 3, using a lowpass-highpass filter pair with transfer functions $H_0(z)$ and $H_1(z)$. Hence, the z -transforms of these signals are expressible as $X_k(z) = H_k(z)X(z)$ for $k = 0, 1$.

After filtering, the signals in both channels are down-sampled by a factor of two by picking up every second sample, resulting in two subband signal components, denoted by $v_0[n]$ and $v_1[n]$ in Figure 3. If the input sampling rate is F_s , then the sampling rates of $v_0[n]$ and $v_1[n]$ are $F_s/2$. The z -transforms of these components are given by

$$V_k(z) = \frac{1}{2} \left[H_k(z^{1/2}) X(z^{1/2}) + H_k(-z^{1/2}) X(-z^{1/2}) \right] \quad \text{for } k = 0, 1. \quad (2)$$

Typically, $H_0(z)$ and $H_1(z)$ have the same transition band region with the band edges being located around $f = F_s/4$ at $f = (1-\rho_1)F_s/4$ and $f = (1+\rho_2)F_s/4$ with $\rho_1 > 0$ and $\rho_2 > 0$, as shown in Figure 4(b). In order to give a pictorial viewpoint of what is happening in the frequency domain, Figure 4(a) shows the Fourier transforms of an input signal $x[n]$, whereas Figure 5 shows those of signals $x_0[n]$, $x_1[n]$, $v_0[n]$, and $v_1[n]$. These transforms are obtained from the corresponding z -transform by simply using the substitution $z = e^{j2\pi f/F_s}$. It is seen that after decimation $V_k(z)$ for $k = 0, 1$ contain two overlapping components $X_k(z^{1/2})$ and $X_k(-z^{1/2})$. This overlapping can, however, be eliminated in the overall system of Figure 3 by properly designing the transfer functions $H_0(z)$, $H_1(z)$, $F_0(z)$, and $F_1(z)$, as will be seen later on.

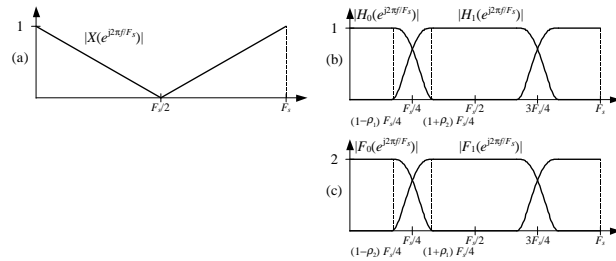


Figure 4. (a) Magnitude of the Fourier transform of an input signal $x[n]$. (b) Amplitude responses for $H_0(z)$ and $H_1(z)$. (c) Amplitude responses for $F_0(z)$ and $F_1(z)$.

2.1.2 Operation of the processing unit

In the processing unit, the signals $v_0[n]$ and $v_1[n]$ are compressed and coded suitably for either transmission or storage purposes. Before using the synthesis part, signals in both channels are decoded. The resulting signals denoted by $w_0[n]$ and $w_1[n]$ in Figure 3 may differ from the original signals $v_0[n]$ and $v_1[n]$ due to possible distortions caused by coding and quantization errors as well as channel impairments. In the sequel, it is supposed, for simplicity, that there are no coding, quantization, or channel degradations, that is, $w_0[n] \equiv v_0[n]$ and $w_1[n] \equiv v_1[n]$.

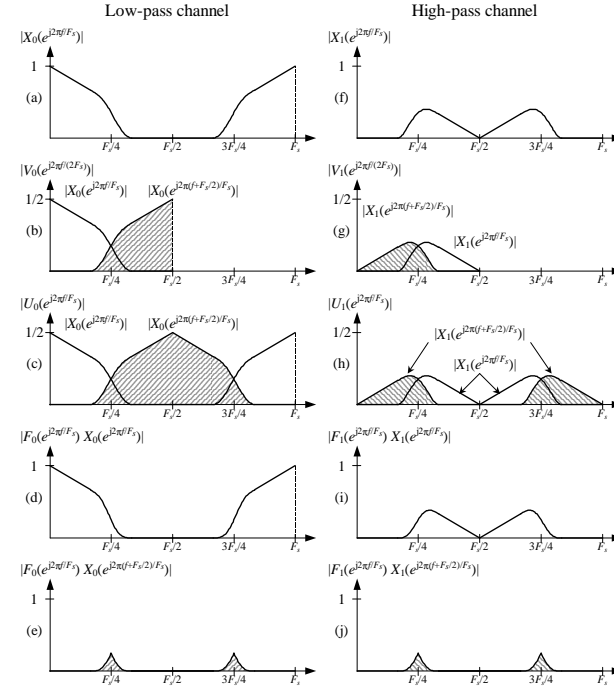


Figure 5. Magnitudes of the Fourier transforms of the signals in the two-channel filter bank of Figure 3. (a), (f) Transforms of $x_0[n]$ and $x_1[n]$. (b), (g) Transforms of $v_0[n]$ and $v_1[n]$. (c), (h) Transforms of $u_0[n]$ and $u_1[n]$. (d), (i) Transforms of unaliased components of $v_0[n]$ and $v_1[n]$. (e), (j) Transforms of aliased components of $v_0[n]$ and $v_1[n]$.

2.1.3 Operation of the synthesis bank

The role of the synthesis bank is to approximately reconstruct in three steps the delayed version of the original signal from the signal components $w_0[n]$ and $w_1[n]$. In the first step, these signals are up-sampled by a factor of two by inserting zero-valued samples between the existing samples yielding two components, denoted by $u_0[n]$ and $u_1[n]$ in Figure 3. In the $w_0[n] \equiv v_0[n]$ and $w_1[n] \equiv v_1[n]$ case, the z -transforms of these signals are expressible as

$$U_k(z) = V_k(z^2) = \frac{1}{2} [X_k(z) + X_k(-z)] \quad \text{for } k = 0, 1. \quad (3)$$

Simultaneously, the sampling rate is increased from $F_s/2$ to F_s and the baseband from $[0, F_s/4]$ to $[0, F_s/2]$. Therefore, $u_0[n]$ and $u_1[n]$ contain in their basebands, in addition to the frequency components of $v_0[n]$ and $v_1[n]$ in their baseband $[0, F_s/4]$, the components in $[F_s/4, F_s/2]$, as illustrated in Figure 5. In Equation (3), $X_k(z)$ is the z -transform of the desired unaliased signal component, whereas $X_k(-z)$ is the z -transform of the unwanted aliased signal component that should be eliminated.

The second step involves processing $u_0[n]$ and $u_1[n]$ by a lowpass–highpass filter pair with transfer functions $F_0(z)$ and $F_1(z)$, whereas the third step is to add the filtered signals, denoted by $y_0[n]$ and $y_1[n]$ in Figure 3, to yield the overall output $y[n]$. The z -transform of $y[n]$ is given by $Y(z) = Y_1(z) + Y_2(z)$, (4)

where

$$Y_k(z) = F_k(z)V_k(z^2) = \frac{1}{2}[F_k(z)X_k(z) + F_k(z)X_k(-z)] \text{ for } k = 0,1. \quad (5)$$

The role of the synthesis filters with transfer functions $F_0(z)$ and $F_1(z)$ is twofold. First, it is desired that $Y(z)$ does not contain the terms $X_0(-z)$ and $X_1(-z)$. This is achieved by requiring that $F_0(z)X_0(-z) = -F_1(z)X_1(-z)$. Second, if it is desired that $y[n]$ is approximately a delayed version of $x[n]$, that is, $y[n] \approx x[n - K]$, then $F_0(z)X_0(z) + F_1(z)X_1(z) \approx z^{-K}X(z)$ should be satisfied.

In order to satisfy these requirements, $F_0(z)$ and $F_1(z)$ should generate a lowpass–highpass filter pair in a manner similar to $H_0(z)$ and $H_1(z)$. There exist two main differences. First, due to the alias-free conditions to be considered in the next subsection, the lower and upper edges of this filter pair are located at $f = (1 - \rho_2)F_s/4$ and $f = (1 + \rho_1)F_s/4$, as shown in Figure 4(c). Second, because of interpolation, the amplitude responses should approximate two in the passbands. The last subfigures on the left and right sides of Figure 5 show how the above conditions can be satisfied in the frequency domain. The exact simultaneous conditions for $H_0(z)$, $H_1(z)$, $F_0(z)$, and $F_1(z)$ to satisfy the above-mentioned two conditions will be given in the following subsections.

2.2 Alias-Free Filter Banks

Combining Equations (1), (4), and (5) the relation between the input and the output signals of Figure 3 is expressible as

$$Y(z) = T(z)X(z) + A(z)X(-z), \quad (6)$$

where

$$T(z) = \frac{1}{2}[H_0(z)F_0(z) + H_1(z)F_1(z)] \quad (7)$$

is the overall distortion transfer function and

$$A(z) = \frac{1}{2}[H_0(-z)F_0(z) + H_1(-z)F_1(z)] \quad (8)$$

is the aliasing transfer function. In order to generate an alias-free filter bank, this term has to be canceled, that is, $A(z) \equiv 0$. The most straightforward way of achieving this is to select $F_0(z)$ and $F_1(z)$ as follows:

$$F_0(z) = 2H_1(-z) \quad (9)$$

$$F_1(z) = -2H_0(-z). \quad (10)$$

In the sequel, these conditions are used except for Subsection 2.5.2 where the filter bank is constructed with the aid of causal and anti-causal IIR filters. After fixing $F_0(z)$ and $F_1(z)$ in the above manner, the input-output relation of Equation (6) takes the following simplified form:

$$Y(z) = T(z)X(z), \quad (11)$$

where

$$T(z) = H_0(z)H_1(-z) - H_0(-z)H_1(z). \quad (12)$$

There are two important reasons for concentrating on the synthesis of two-channel filter banks in such a manner that they are alias-free. First, relating $F_0(z)$ and $F_1(z)$ to $H_0(z)$ and $H_1(z)$ according to Equations (9) and (10) makes both the design and implementation of the overall system more efficient compared to the nearly alias-free case. Second, it has been observed that when synthesizing the bank without the exact alias-free condition leads to a system that is practically alias-free. This fact can be seen, for instance, from the results given by Nayebi, Barnwell III, and Smith in (1992).

2.3 Perfect-Reconstruction (PR) and Nearly Perfect-Reconstruction (NPR) Filter Banks

The following subsection states the necessary and sufficient conditions for an FIR two-channel filter bank to satisfy the PR conditions and describes their connections to the linear-phase half-band FIR filters. Furthermore, these conditions are extended to their IIR counterparts.

2.3.1 Theorem for the PR Property

The PR property, that is, $y[n] = x[n - K]$, is the ability of a system to produce an output signal that is a delayed replica of the input signal. The necessary conditions for the PR property are given for a two-channel FIR filter bank by the following theorem:

Theorem for the PR property: Consider the alias-free two-channel filter bank shown in Figure 3 with $w_0[n] \equiv v_0[n]$ and $w_1[n] \equiv v_1[n]$ and let $H_0(z)$ and $H_1(z)$ be the transfer functions of FIR filters given by $H_0(z) = \sum_{n=0}^{N_0} h_0[n]z^{-n}$ and $H_1(z) = \sum_{n=0}^{N_1} h_1[n]z^{-n}$. Then, $y[n] = x[n - K]$ with K being an odd integer, that is, $T(z) = z^{-K}$, is met provided that the impulse-response coefficients of

$$E(z) = H_0(z)H_1(-z) = \sum_{n=0}^{N_0+N_1} e[n]z^{-n} \quad (13)$$

satisfy

$$e[n] = \begin{cases} 1/2 & \text{for } n = K \\ 0 & \text{for } n \text{ is odd and } n \neq K. \end{cases} \quad (14)$$

In order to prove this theorem, Equation (12) is rewritten as

$$T(z) = \sum_{n=0}^{N_0+N_1} t[n]z^{-n} = E(z) + [-E(-z)] = \sum_{n=0}^{N_0+N_1} (e[n] + \hat{e}[n])z^{-n}, \quad (15)$$

where

$$\hat{e}[n] = \begin{cases} -e[n] & \text{for } n \text{ even} \\ e[n] & \text{for } n \text{ odd}. \end{cases} \quad (16)$$

The impulse-response coefficients of this $T(z)$ satisfy

$$t[n] = e[n] + \hat{e}[n] = \begin{cases} 1 & \text{for } n = K \\ 0 & \text{for } n \neq K, \end{cases} \quad (17)$$

yielding

$$T(z) = E(z) - E(-z) = z^{-K}. \quad (18)$$

This implies that the output signal is the replica of the input signal delayed by K samples, as is desired.

It is well known that the PR property can be satisfied only when K is an odd integer and N_0+N_1 is two times an odd integer (see, e.g., (Vaidyanathan, 1993)). There are two basic alternatives to achieve the PR property, namely, $K=(N_0+N_1)/2$ and $K < (N_0+N_1)/2$, as illustrated in Figures 6(a) and 6(b), respectively. In the first case, $E(z)$ is an FIR filter transfer function with a symmetric impulse response and the impulse-response value occurring at the odd central point $n=K$ being equal to $1/2$, whereas the other values occurring at odd values of n are zero. Hence, $E(z)$ is the transfer function of a linear-phase FIR half-band filter (see, e.g., (Saramäki, 1993)). In the second case, the impulse-response values at odd values of n are also zero except for one odd value $n=K$, where the impulse response takes on the value of $1/2$. The $K=(N_0+N_1)/2$ case is attractive when the overall delay of K samples is tolerable, whereas the $K < (N_0+N_1)/2$ case is used for reducing the delay caused by the filter bank to the overall signal.

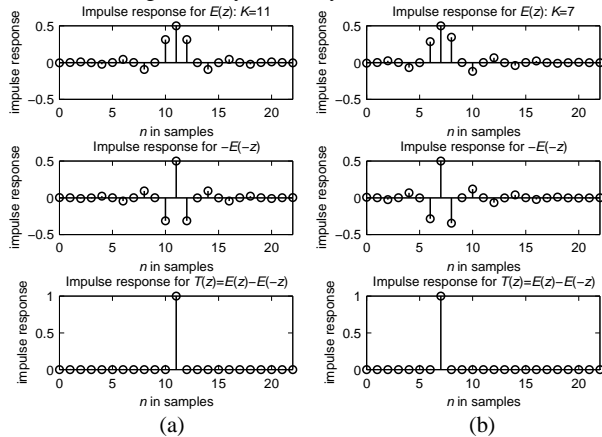


Figure 6. Impulse responses for $E(z)$, $E(-z)$, and $T(z)$ for PR filter banks with $N_0+N_1=22$. (a) $K=11=(N_0+N_1)/2$. (b) $K=7 < (N_0+N_1)/2$.

In the PR case, there is no amplitude or phase distortion. This is due to the fact that $t[n]$ is nonzero only at $n=K$ achieving the value of unity. In the NPR case, the impulse response values $t[n]$ differ slightly from zero for $n \neq K$ and slightly from 1 for $n=K$ so that there exists some amplitude and/or phase distortions. These distortions are tolerable in many practical applications (lossy channel coding and quantization) provided that they are smaller than the errors introduced in the processing unit. Moreover, by slightly releasing the PR condition, filter banks with better selectivities can be synthesized, as will be seen later on.

The above criteria for the PR and NPR property are also valid for IIR filter banks to be considered in Subsection 2.5 (except for the banks to be described in Subsection 2.5.1). The main difference is that the impulse responses of IIR analysis filters are of infinite length. Therefore, the impulse response $e[n]$ of $E(z)$ and the response $t[n]$ of $T(z)$ are also of infinite length. For a PR system $e[n]$ and $t[n]$ must satisfy the conditions of Equations (14) and (17) for $0 \leq n < \infty$, whereas in the NPR case these conditions should be approximately satisfied.

2.3.2 PR Filter Bank Design and the Theorem for the PR Reconstruction

Consider

$$E(z) = \sum_{n=0}^{N_0+N_1} e[n]z^{-n} = S \prod_{k=1}^{N_0+N_1} (1 - z_k z^{-1}) \quad (19)$$

with the impulse-response coefficients satisfying the conditions of Equations (14). The factorization of $E(z)$ as $E(z) = H_0(z)H_1(-z)$ can be performed as follows. First, the zeros z_k of $E(z)$ for $k=1,2,\dots,N_0+N_1$ are divided into two groups α_k for $k=1,2,\dots,N_0$ and β_k for $k=1,2,\dots,N_1$ in such a manner that the zeros in both groups are either real or occur in complex-conjugate pairs. Second, the constant S of $E(z)$ is factorized as $S = S_0S_1$. Then, according to the theorem of the previous subsection, the transfer functions given by

$$H_0(z) = \sum_{n=0}^{N_0} h_0[n]z^{-n} = S_0 \prod_{k=1}^{N_0} (1 - \alpha_k z^{-1}) \quad (20)$$

$$\hat{H}_1(z) \equiv H_1(-z) = \sum_{n=0}^{N_1} \hat{h}_1[n]z^{-n} = S_1 \prod_{k=1}^{N_1} (1 - \beta_k z^{-1}) \quad (21)$$

can be used for generating a PR two-channel filter bank. In the above, $H_0(z)$ is directly the transfer function of the lowpass analysis filter. The corresponding highpass filter transfer function $H_1(z)$ is obtained from $\hat{H}_1(z)$ by selecting the impulse-response coefficients to be $h_1[n] = (-1)^n \hat{h}_1[n]$ for $n=0,1,\dots,N_1$. The amplitude responses of these two filters are related through $|H_1(e^{j\omega})| = |\hat{H}_1(e^{j(\pi-\omega)})|$ so that $\hat{H}_1(z)$ and $H_1(z)$ form a lowpass-highpass filter pair with the amplitude responses obtained from each other using a lowpass-to-highpass transformation $\omega \rightarrow \pi - \omega$.

According to the above discussion, the synthesis of a PR two-channel filter bank can be stated as follows: Given an odd integer K and integers N_0 and N_1 such that their sum is two times an odd integer, find $E(z)$ of order N_0+N_1 such that its impulse-response coefficients satisfy the conditions of Equation (14) and $H_0(z)$ and $H_1(z)$ generated using the above factorization scheme form a lowpass-highpass filter pair with the desired properties.

In general, this problem statement cannot be exploited in a straightforward manner for designing two-channel FIR filter banks. However, there are two exceptional cases. In the first case, $K=(N_0+N_1)/2$ and this problem statement is widely used for designing start-up two-channel filter banks for generating discrete-time wavelet banks (Vetterli and Herley, 1992; Vetterli and Kovačević 1995; Misiti et al., 1996). In this case, half-band linear-phase FIR filter transfer functions $E(z)$ with the maximum numbers of zeros at $z=-1$ are of great importance. As a curiosity, these filters are special cases of the maximally flat FIR filters introduced by Herrmann (1971).

In the second exceptional case, the impulse-response coefficients of $H_0(z)$ and $\hat{H}_1(z)$ are time-reversed version of each other, that is, $\hat{h}_1[n] = h_0[N_0 - n]$ for $n=0,1,\dots,N_0$ (see Figure 7). Furthermore $N_0=N_1=K$. These conditions imply the following (see, e.g., (Herrmann and Schussler, 1970; Saramäki, 1993)). If $H_0(z)$ has a real zero or a complex-conjugate zero pair inside (outside) the unit circle, then $\hat{H}_1(z)$ has a reciprocal real zero or a complex-conjugate zero pair outside (inside) the unit circle. Most importantly, if $H_0(z)$ has zeros on the unit circle, then $\hat{H}_1(z)$ has the same zeros on the unit circle meaning that $E(z) = H_0(z)\hat{H}_1(z)$ is a linear-phase

half-band FIR filter with the restriction that the zeros occurring on the unit circle are double zeros (see Figure 7). Furthermore, $|E(e^{j\omega})| = |H_0(e^{j\omega})|^2 = |\hat{H}_1(e^{j\omega})|^2$.

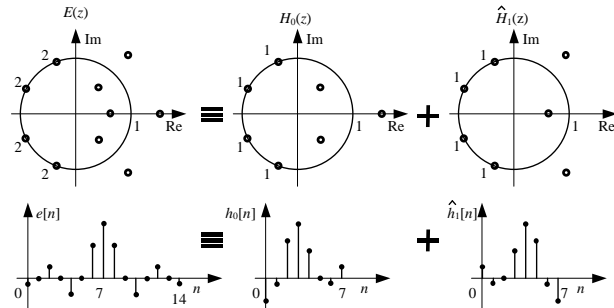


Figure 7. Factorization of a half-band $E(z)$ having double zeros on the unit circle into $H_0(z)$ and $\hat{H}_1(z)$ having time-reversed impulse responses.

This alternative for constructing PR FIR two-channel filter banks, called later on in this chapter as orthogonal banks, was independently observed by Mintzer (Mintzer, 1985) and Smith and Barnwell (Smith, 1986). In their design schemes, $E(z)$ of order $2N_0$ having double zeros on the unit circle is designed to exhibit an equiripple amplitude response in the stopband $[\omega_s, \pi]$ with $\omega_s > \pi/2$. The actual synthesis is performed by first designing, by means of the Remez algorithm (McClellan, Parks, and Rabiner 1973), a conventional half-band filter of the same order to have a minimax behavior in the same stopband. Then, the coefficients of this filter are modified to give a rise to the desired half-band filter. After knowing $E(z)$, all what is needed is to share the zeros between $H_0(z)$ and $\hat{H}_1(z)$ as described above (see Figure 7) as well as to factorize S as $S = S_0 S_1$ so that the resulting impulse responses are time-reversed versions of each other. This technique results in analysis transfer functions $H_0(z)$ and $H_1(z)$ such that the maximum amplitude value of $H_0(z)$ [$H_1(z)$] in the stopband $[\omega_s, \pi]$ ($[0, \pi - \omega_s]$) is $\sqrt{\delta_s}$ with δ_s being the stopband ripple of $E(z)$.

2.4 FIR Filter Banks and Their Design

This subsection reviews the synthesis of various two-channel filter banks where both $H_0(z)$ and $H_1(z)$ are transfer functions of FIR filters as given by

$$H_0(z) = \sum_{n=0}^{N_0} h_0[n] z^{-n} \quad (22)$$

$$H_1(z) = \sum_{n=0}^{N_1} h_1[n] z^{-n} \quad (23)$$

Moreover, in order to obtain an alias-free system, $F_0(z)$ and $F_1(z)$ are also FIR filters satisfying Equations (9) and (10).

2.4.1 FIR Filter Bank Classification

Alias-free two-channel FIR filter banks can be classified into several filter bank types according to Table I. The type depends first on the relation between the analysis transfer functions $H_0(z)$ and $H_1(z)$, second on whether these transfer functions are linear-phase FIR filters or not, and third on whether the PR or NPR property is desired to be achieved. In addition to these properties, Table I shows for each type the number of unknowns to be optimized, whether the order(s) must be odd or even, and the relation of the overall filter bank delay to the filter orders. Filter banks with the filter bank delay less than N_0 (for QMF banks) and $(N_0+N_1)/2$ (for biorthogonal banks) are later on referred to as low-delay two-channel filter banks.

Table I Classification of two-channel FIR filter banks

Filter bank type	Filter relation	Phase	Filter order	Number of unknowns	Filter bank delay	PR
QMF	$H_1(z) = H_0(-z)$	linear-phase	odd	$(N_0+1)/2$	N_0	NPR
		nonlinear-phase		N_0+1	$< N_0$	
Orthogonal	$H_1(z) = -z^{-N_0} H_0(-z^{-1})$	nonlinear-phase	odd	N_0+1	N_0	PR NPR
Biorthogonal	$H_0(z), H_1(z)$	linear-phase	odd-odd	$(N_0+N_1)/2+1$	$(N_0+N_1)/2$	PR NPR
			even-even	$(N_0+N_1)/2+2$		
		nonlinear-phase	odd-odd	N_0+N_1+2	$< (N_0+N_1)/2$	
			even-even			

In the following subsections the definition of each filter bank type is given in more details along with their properties and a short review of the existing synthesis schemes. Examples comparing the various filter types with each other will be given in Subsection 2.4.7. We start by stating a general optimization problem including all FIR filter banks of Table I.

2.4.2 General FIR Filter Bank Design Problem

It has turned out to be beneficial to state a general optimization problem including all the filter types of Table I as follows (Bregović and Saramäki, 1999, 2000b): Given the type of two-channel filter bank, the filter orders N_0 and N_1 , the passband and stopband band frequencies $\omega_p^{(0)} < \pi/2$ and $\omega_s^{(0)} > \pi/2$ for $H_0(z)$ as well as $\omega_p^{(1)} > \pi/2$ and $\omega_s^{(1)} < \pi/2$ for $H_1(z)$, the reconstruction error δ_a , and the passband ripple δ_p as well as the filter bank delay K , find the adjustable coefficients of $H_0(z)$ and $H_1(z)$, as given by Equations (22) and (23), to minimize

$$\varepsilon = \max \left(\int_{\omega_s^{(0)}}^{\pi} |H_0(e^{j\omega})|^2 d\omega, \int_0^{\omega_s^{(1)}} |H_1(e^{j\omega})|^2 d\omega \right) \quad (24)$$

subject to

$$\max_{\omega \in (0, \omega_p^{(0)})} \left| |H_0(e^{j\omega})| - 1 \right| \leq \delta_p \quad \text{and} \quad \max_{\omega \in (\omega_p^{(1)}, \pi)} \left| |H_1(e^{j\omega})| - 1 \right| \leq \delta_p, \quad (25)$$

$$\max_{\omega \in (\omega_p^{(0)}, \omega_s^{(0)})} \left| |H_0(e^{j\omega})| - 1 \right| \leq \delta_p \quad \text{and} \quad \max_{\omega \in (\omega_s^{(1)}, \omega_p^{(1)})} \left| |H_1(e^{j\omega})| - 1 \right| \leq \delta_p, \quad (26)$$

and

$$\max_{\omega \in [0, \pi]} \left| T(e^{j\omega}) - e^{-jK\omega} \right| \leq \delta_a, \quad (27)$$

where

$$T(e^{j\omega}) = H_0(e^{j\omega})H_1(e^{j(\omega+\pi)}) - H_0(e^{j(\omega+\pi)})H_1(e^{j\omega}). \quad (28)$$

The main objective is to minimize the maximum of the stopband energies of $H_0(z)$ and $H_1(z)$ subject to some constraints, as illustrated in Figure 8. First, the amplitude responses of both $H_0(z)$ and $H_1(z)$ have to stay in the passband within the given limits $1 \pm \delta_p$. Second, the maximum allowable value for these amplitude responses in the transition bands is $1 + \delta_p$. Third, the maximum of the absolute value of the deviation between the overall frequency response and the constant delay of K samples has to be in the overall frequency range less than or equal to δ_a . For the PR filter banks, this deviation is zero. As will be seen later, some of the constraints are automatically satisfied by some of the above-mentioned types of two-channel filter banks.

The above optimization problem has been stated in terms of the angular frequency ω that is related to the "real" frequency f and the sampling rate F_s through $\omega = 2\pi f/F_s$. The problem formulation is very general. For instance, the band edges for $H_0(z)$ and $H_1(z)$ can be selected arbitrarily unlike in the case of Figure 4(b), where the edges for $H_0(z)$ and $H_1(z)$ are the same. The special feature of the problem statement is that the maximum of the stopband energies of the two filters is minimized, allowing us to treat both filters in a similar manner. In most other existing statements the sum of these energies is minimized. The above problem has been stated in such a manner that the optimum solution can be found using a two step-procedure proposed in Bregović and Saramäki (1999, 2000b). In the first step, a good starting-point filter bank for further optimization is generated using a simple design scheme for the selected filter bank type. The second step involves optimizing the filter bank with the aid of an efficient constrained nonlinear optimization algorithm (Dutta, 1977; Saramäki, 1998).

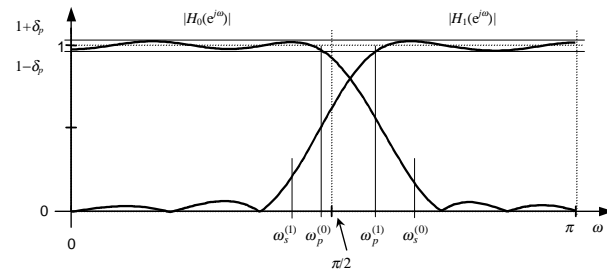


Figure 8. Specifications for $H_0(z)$ and $H_1(z)$.

2.4.3 NPR Quadrature Mirror Filter (QMF) Banks

Quadrature mirror filter (QMF) banks were the first type of filter banks used in signal processing applications for separating signals into subbands and for reconstructing them from individual subbands (Esteban and Galand, 1977). For a QMF bank, $H_1(z) = H_0(-z)$ so that $H_0(z)$, as given by Equation (22), is the only transfer function to be optimized. In this case, $T(z)$, as given by Equation (12), becomes

$$T(z) = \sum_{n=0}^{2N_0} t[n]z^{-n} = [H_0(z)]^2 - [H_0(-z)]^2. \quad (29)$$

This transfer function is desired to approximate the delay z^{-K} with K being an odd integer satisfying $K \leq N_0$. It is well-known that in this case the PR property cannot be satisfied except for the trivial case with $H_0(z) = (1+z^{-1})/2$ that does not provide good attenuation characteristics (Vaidyanathan, 1993).

Using the decomposition $H_0(z) = G_0(z^2) + z^{-1}G_1(z^2)$, the overall bank can be effectively implemented as shown in Figure 9 (Malvar, 1992a). According to Table I, there are two types of QMF banks to be considered next.

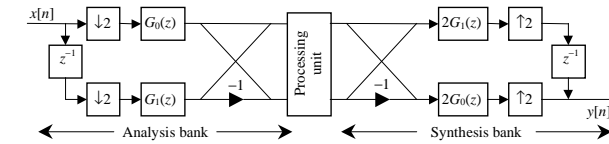


Figure 9. Efficient implementation for a QMF two-channel bank.

2.4.3.1 QMF banks with linear-phase subfilters.

For these banks, the impulse-response coefficients of $H_0(z)$ possess an even symmetry, that is, $h_0[N_0 - n] = h_0[n]$ for $n = 0, 1, \dots, (N_0 - 1)/2$ and $K = N_0$. Hence, for the overall filter bank, there are only $(N_0 + 1)/2$ unknowns. Based on the linear-phase property of $H_0(z)$, the transfer function between the output and input of the overall system has also an impulse response of an even symmetry, that is, $t[2N_0 - n] = t[n]$ for $n = 0, 1, \dots, N_0 - 1$ in Equation (29). Hence, it suffers only from the amplitude distortion.

The first systematic approach for synthesizing QMF banks was proposed by Johnston (Johnston, 1980). In his synthesis technique, the weighted sum of the filter stopband energy and the integral of $\left[|T(e^{j\omega})| - 1 \right]^2$ over the band $[0, \pi/2]$ is minimized. The resulting reconstruction error is not equiripple. An iterative technique resulting in an equiripple reconstruction error has been proposed by Chen and Lee (1992). Further generalizations of this method described by Lim, Yang, and Koh (1993), and Goh, Lim, and Ng (1999a) enable us to obtain also equiripple behaviors in the filter stopbands. It has turned out that in many applications it is beneficial to design filter banks in such a way that the reconstruction error exhibits an equiripple (minimax) behavior, whereas the stopband energies of the filters are minimized (Bregović and Saramäki 1999, 2000b). This problem can be solved conveniently using the general problem statement described in Subsection 2.4.2 as well as the two-step optimization scheme mentioned in the same subsection. In this case, the problem takes a simplified form since the stopband energies of both filters are the same and there is no need to control the passband and transition band behaviors. All what is needed is to find a good start-up solution. For this purpose, efficient iterative methods described by Xu, Lu, and Antoniou (1998) and Lu, Xu, and Antoniou (1998) can be used. It should be emphasized that the proper use of constrained optimization algorithms guarantees the convergence at least to a good local optimum solution. However, if such an algorithm together with a good initial solution is not available, then iterative methods are of a practical value. This

is because they give in many cases with a small computation workload a satisfactory sub-optimal solution.

2.4.3.2 Low-delay OMF banks with nonlinear-phase subfilters.

In this case, $H_0(z)$ is a nonlinear-phase filter. Hence, all the impulse-response values $h_0[n]$ for $n=0, 1, \dots, N_0$ are unknowns. The filter bank delay K is no more equal to the filter order N_0 . This enables us to increase the filter orders to improve the filter banks performance without increasing the overall filter bank delay.

The reconstruction error is now given by

$$\left| T(e^{j\omega}) - e^{-jK\omega} \right| = \left| \left[H_0(e^{j\omega}) \right]^2 - \left[H_0(e^{j(\omega+\pi)}) \right]^2 - e^{-jK\omega} \right|, \quad (30)$$

that is desired to be made small in the overall baseband $[0, \pi]$. Due to the nonlinear-phase characteristics, the performance of $H_0(z)$ in the passband must also be controlled unlike for the linear-phase case, where a good stopband characteristics together with a small overall amplitude distortion automatically guarantees that the passband amplitude response of $H_0(z)$ approximates unity with a small tolerance.

Similar to the linear-phase QMF banks, iterative methods described by Xu et al. (1998) and Lu et al. (1998) exist for designing low-delay QMF banks. These filter banks can be used as start-up solutions for the general optimization problem stated in Subsection 2.4.2. For this problem, the stopband energy of only one filter has to be minimized, but all the remaining constraints must be included.

2.4.4 PR Orthogonal Filter Banks

These filter banks were considered in Subsection 2.3.2. According to this discussion, the relation between the analysis filters is defined as

$$H_1(z) = -z^{-N_0} H_0(-z^{-1}), \quad (31)$$

where $H_0(z)$ is given by Equation (22) and N_0 , the filter order, is an odd integer. This makes the impulse response coefficients of $H_0(z)$ and $H_1(-z)$ time-reversed versions of each other, that is, $h_1[n] = (-1)^n \cdot h_0[N_0 - n]$ for $n=0, 1, \dots, N_0$. Furthermore, the PR property implies that in this case the following conditions are satisfied:

1. $E(z) = H_0(z)H_1(-z)$ is a linear-phase half-band FIR filter of order $2N_0$.
2. The zeros of $E(z)$ occurring on the unit circle are double zeros.

As was pointed out in Subsection 2.3.2, this enables us to factorize $E(z)$ into two transfer functions $H_0(z)$ and $H_1(-z)$ of order N_0 in such a manner that their impulse response are time-reversed versions of each other and the amplitude response of the corresponding $H_1(z)$ is related to that of $H_0(z)$ through $|H_1(e^{j\omega})| = |H_0(e^{j(\pi-\omega)})|$. In Subsection 2.3.2, a synthesis scheme was briefly described for designing $H_0(z)$ and $H_1(z)$ to exhibit minimax amplitude behaviors in the stopbands. For designing corresponding filters with least-mean-square error behaviors in the stopbands, the most efficient way is to use iterative algorithms described by Blu (1998) and Bregović and Saramäki (2000a). These algorithms are fast and the convergence to the optimum solution is independent of the initial solution.

Besides of the direct form implementation of Figure 3, orthogonal filter banks can be also realized using a lattice form as shown in Figure 10. This structure is a slightly modified version of those proposed by Vaidyanathan and Hoang (1988). For a given odd order N_0 , there are $(N_0+1)/2$ unknown lattice coefficients α_k as well as the scaling constants β and 2β . The role of the scaling constants is to make the amplitude responses of the analysis and synthesis filters to

approximate one and two in their passband regions, respectively. The advantage of using a lattice structure is that the PR property is satisfied for any combination of the lattice coefficients that is very attractive in the case of coefficient quantization. For the conversion between the lattice coefficients and the original coefficients, see Vaidyanathan and Hoang (1988) and Goh and Lim (1999b).

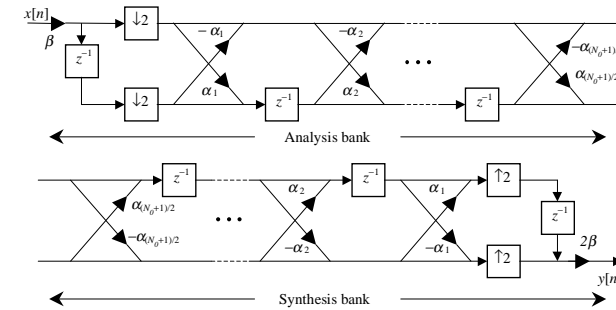


Figure 10. Lattice structure for orthogonal filter banks.

2.4.5 PR Biorthogonal Filter Banks

For biorthogonal filter banks, $H_0(z)$ and $H_1(z)$ are different transfer functions being related to each other through the PR property. According to the linear-phase property of the filters, they are divided into two types (see Table I), namely, filter banks with linear-phase subfilters and filter banks with nonlinear-phase subfilters. These two types will be considered next.

2.4.5.1 PR biorthogonal filter banks with linear-phase subfilters.

For PR biorthogonal filter banks with linear-phase subfilters, $H_0(z)$ and $H_1(z)$ satisfy the following conditions:

1. The impulse responses of $H_0(z)$ and $H_1(-z)$ possess an even symmetry, meaning that the coefficients of $H_0(z)$ and $H_1(z)$ satisfy $h_0[N_0 - n] = h_0[n]$ for $n=0, 1, \dots, N_0$ and $h_1[N_1 - n] = (-1)^{N_1} \cdot h_1[n]$ for $n=0, 1, \dots, N_1$, respectively (for N_1 even (odd), the impulse response of $H_1(z)$ possesses an even (odd) symmetry).
2. The sum of the filter orders N_0 and N_1 is two times an odd integer, that is, $N_0 + N_1 = 2K$ with K being an odd integer.
3. $E(z) = H_0(z)H_1(-z)$ is a half-band linear-phase FIR filter of order $N_0 + N_1$.

There exist only the following two cases to meet these conditions:

- Case A: N_0 and N_1 are odd integers and their sum is two times an odd integer K .
- Case B: N_0 and N_1 are even integers and their sum is two times an odd integer K .

In both cases, the filter bank delay is $K = (N_0 + N_1)/2$.

The first effective iterative algorithm for designing biorthogonal filter banks has been proposed by Hornig and Willson (1992). An iterative algorithm giving rise to analysis filters exhibiting equiripple amplitude performances in their stopbands has been proposed by Yang, Lee, and Chieu (1998). The results of the above-mentioned algorithms can be used as start-up solutions for the general optimization problem stated in Subsection 2.4.2. In this case, all the constraints are needed. It has turned out that, instead of using $\delta_i = 0$ in Equation (27), $\delta_i = 10^{-13}$ gives a very accurate solution.

For implementing biorthogonal filter banks, like in the case of the orthogonal banks, there exists also a lattice structure as shown in Figure 11 (Nguyen and Vaidyanathan, 1989) that can be used in some cases (Vaidyanathan, 1993). The coefficient values for the lattice structure can be found by direct optimization (Vaidyanathan, 1993) or by transforming the optimized direct-form coefficients to those used in the lattice structure (Nguyen, 1992b, 1995).

A very useful alternative for designing and implementing biorthogonal two-channel filter banks is to use the lifting scheme that was introduced by Sweldens (1996) and Daubechies and Sweldens (1998) for designing biorthogonal two-channel banks for generating discrete-time wavelet banks. As shown by Daubechies and Sweldens (1998), any PR biorthogonal and orthogonal two-channel filter bank can be implemented using this technique. The main advantage of the resulting structure is that the PR property is still remaining after the quantization of the lifting coefficients into very simple representation forms (without any extra scaling). When applying the lifting scheme for designing biorthogonal two-channel filter banks, a PR filter bank with short analysis and synthesis filters is used as a starting point. After that, PR filter banks with higher filter orders are successively generated applying the so-called lifting and dual lifting steps. For more details, see Sweldens (1996) and Daubechies and Sweldens (1998). The lifting scheme has been also used for designing cosine-modulated low-delay biorthogonal filter banks by Karp and Mertins (1997).

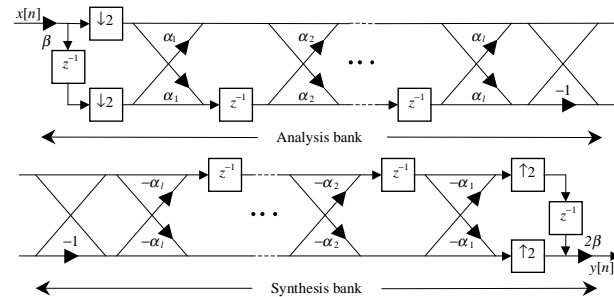


Figure 11. Lattice structure for biorthogonal filter banks.

2.4.5.2 Low-delay PR biorthogonal filter banks with nonlinear-phase subfilters.

For low-delay PR biorthogonal filter banks with nonlinear-phase subfilters, $H_0(z)$ and $H_1(z)$ satisfy the following conditions:

1. The impulse responses of $H_0(z)$ and $H_1(z)$ are not symmetric.
2. The impulse response of $E(z) = H_0(z)H_1(-z) = \sum_{n=0}^{N_0+N_1} e[n]z^{-n}$ satisfies

$$e[n] = \begin{cases} 1/2 & \text{for } n = K \\ 0 & \text{for } n \text{ is odd and } n \neq K, \end{cases} \quad (32)$$

where K is an odd integer with $K < (N_0 + N_1)/2$.

An example for an impulse response of $E(z)$ is shown on Figure 6(b). The second condition implies that the overall transfer function between the output and input is $T(z) = z^{-K}$ with K less than $(N_0 + N_1)/2$. The sum of the filter orders must be two times an odd integer. Since the overall system delay is less than half the sum of the filter orders, the impulse responses of $H_0(z)$ and

$H_1(z)$ cannot possess symmetries. Due to the nonlinearity, all the impulse response values are unknowns. The high number of unknowns (altogether N_0+N_1+2) and the PR condition with the delay less than half the sum of the filter orders makes the synthesis of the overall system very nonlinear and complicated.

Low-delay PR biorthogonal filter banks have been first introduced by Nayebi, Barnwell, and Smith (1992, 1994). The filter banks obtained by using their design scheme are suboptimal, as has been shown in some later papers. However, they have made several important observations concerning the properties of low-delay filter banks. First, it is not advisable to design filter banks with a very small delay compared to the filter orders. The efficiency of such systems is low in the sense that after certain filter orders for the same overall delay, the use of larger filter orders result only in a negligible improvement in the performance of the filter bank. Second, additional constraints are necessary in the transition bands of the filters due to the artifacts often occurring in these bands.

Similar to the linear-phase case for designing this type of filter banks, to obtain a good result, the problem formulation according to Subsection 2.4.2 together with a two-step design method described there is recommended. In this case, a good initial solution is obtained using an iterative method described by Abdel-Raheem, El-Guibaly, and Antoniou in (1996). Other methods for designing low-delay PR biorthogonal filter banks have been proposed by Schuller and Smith (1995, 1996).

2.4.6 Generalized NPR Filter Banks

As mentioned earlier, it is beneficial in many cases to release the PR condition until the errors caused by the non-idealities of the filter bank to the signal are lower than those caused by the processing unit. The ultimate goal is to achieve better filter bank properties. According to Table I, there are two types of NPR banks that will be considered next.

2.4.6.1 NPR filter banks with linear-phase subfilters.

For an NPR filter bank with linear-phase subfilters, $H_0(z)$ and $H_1(z)$ satisfy the same conditions as for the corresponding PR bank (see Subsection 2.4.5.1) with the exception that now in Condition 3 $E(z) = H_0(z)H_1(-z) = \sum_{n=0}^{N_0+N_1} e[n]z^{-n}$ is nearly a half-band linear-phase FIR filter of order $N_0 + N_1$, that is, its impulse response coefficients satisfy

$$e[n] \approx \begin{cases} 1/2 & \text{for } n = K \\ 0 & \text{for } n \text{ is odd and } n \neq K, \end{cases} \quad (33)$$

where $K = (N_0 + N_1)/2$.

Consequently, the overall transfer function $T(z)$ approximates the delay term z^{-K} . Like for the QMF banks with linear-phase subfilters, the impulse-response coefficients of $T(z)$ possess an even symmetry so that the reconstruction error consists only of an amplitude error. The actual design of these filters can be accomplished by first stating the optimization problem according to Subsection 2.4.2 and then solving the problem with the aid of the two-step design technique mentioned in the same subsection. As an initial solution for the second step, the corresponding PR filter bank can be used.

2.4.6.2 Low-delay NPR filter banks with nonlinear-phase subfilters.

For a low-delay NPR filter bank with nonlinear-phase subfilters, $H_0(z)$ and $H_1(z)$ satisfy the following conditions:

1. The impulse responses of $H_0(z)$ and $H_1(z)$ are not symmetric.
2. The impulse response of $E(z) = H_0(z)H_1(z) = \sum_{n=0}^{N_0+N_1} e[n]z^{-n}$ satisfies

$$e[n] \approx \begin{cases} 1/2 & \text{for } n = K \\ 0 & \text{for } n \text{ is odd and } n \neq K, \end{cases} \quad (34)$$

where K is an odd integer with $K \leq (N_0 + N_1)/2$.

The optimization of these banks can be performed like for the corresponding banks with linear-phase subfilters. The difference is that now the reconstruction error consists of both amplitude and phase errors.

2.4.7 FIR filter bank examples

This subsection compares, in terms of examples, various FIR filter banks considered in this section. An overview of all designs under consideration is given in Table II. For all filter banks, the filter bank delay is $K=31$ and the passband and stopband edges are located at $\omega_p^{(0)} = \omega_s^{(1)} = 0.414\pi$ and $\omega_s^{(0)} = \omega_p^{(1)} = 0.586\pi$. For the banks with linear-phase subfilters and for the orthogonal banks, the orders of both $H_0(z)$ and $H_1(z)$ are $N_0 = N_1 = 31$. For the low-delay banks, $N_0 = N_1 = 63$. Additionally, in the low-delay NPR biorthogonal case, the solution for $N_0 = N_1 = 33$ is also included. For the biorthogonal banks, Table II shows δ_p , the allowable passband ripple of $H_0(z)$ and $H_1(z)$ as well the maximum allowable overshoot in the transition band, and δ_a , the allowable reconstruction error for NPR banks. Furthermore, the table shows the figure where amplitude responses of the analysis filters of the corresponding filter bank are given. For the NPR banks, the reconstruction error is also included in the figures.

Figure 12(a) shows how the amplitude responses of the analysis filters of a QMF bank can be improved compared to the Johnston 32D design (Johnston, 1980) given in Figure 12(b) by minimizing the stopband energies of the filters subject to the maximum reconstruction error of the Johnston design. As seen from Figure 12(a), this optimization approach results in a minimax reconstruction error. As illustrated in Figure 13, the channel selectivity can further be improved for the same filter bank delay by using, instead of linear-phase filters, nonlinear-phase filters of higher orders.

Figures 14(a) and 14(b) compare orthogonal filter banks where the stopband behaviors of the analysis filters have been optimized in the least-mean-square and minimax senses, respectively. As can be expected, the attenuations provided by the filters designed in the least-mean-square sense are lower near the stopband edges, but become higher for frequencies further away from the edges.

Table II FIR filter bank examples

Filter bank type	PR	Phase	N_0	δ_p	δ_a	Figure	Design
QMF	NPR	linear-phase	31	-	$3.23 \cdot 10^{-3}$	Figure 12	(a) minimax
		low-delay	63	-		Figure 13	low-delay
Orthogonal	PR	nonlinear	31	-	0	Figure 14	(a) least-squares (b) minimax
		linear-phase	31	0.01	0	Figure 15	(a) linear-phase (b) low-delay
Biorthogonal	PR	linear-phase	31	0.01		0	Figure 16
		low-delay	63	0.1	Figure 17		
	NPR	linear-phase	31	0.1		10^{-3}	Figure 16
		low-delay	33	0.01	10^{-5}	(a) $N_0 = 33$ (b) $N_0 = 63$	

Figures 15(a) and 15(b) provide a comparison between a linear-phase and a low-delay PR biorthogonal filter bank, respectively. For designing these filters, the overall problem has been stated according to Subsection 2.4.2 and the two-step optimization scheme mentioned there has been used. As can be expected, the stopband attenuations of the analysis filters in the low-delay filter bank are higher due to their higher orders.

Figure 16 shows the amplitude responses of the analysis filters as well as the reconstruction errors for two NPR biorthogonal two-channel filter banks with linear-phase subfilters. It is clearly seen that a larger allowable reconstruction error results in higher stopband attenuations. NPR low-delay biorthogonal two-channel filter banks with nonlinear-phase subfilters provide higher attenuations even with a smaller passband ripple (see Table II) as shown in Figure 17. This figure shows the amplitude characteristics of the analysis filters and the reconstruction errors for filter banks with two different filter orders.

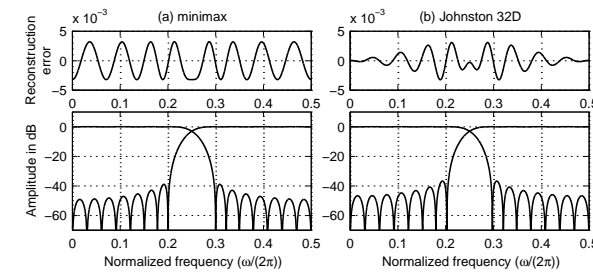


Figure 12. QMF banks with linear-phase filters.

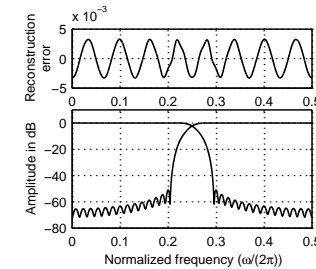


Figure 13. Low-delay QMF bank.

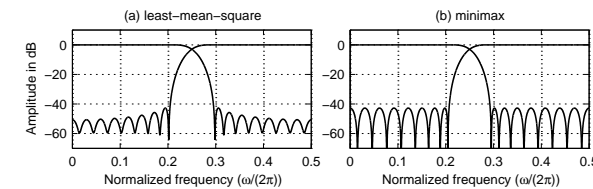


Figure 14. PR orthogonal filter banks.

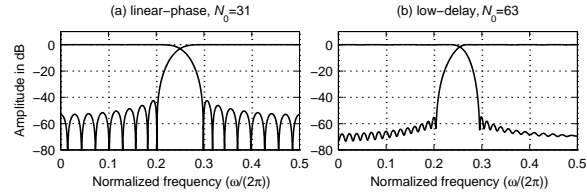


Figure 15. PR biorthogonal filter banks with linear-phase and nonlinear-phase filters.

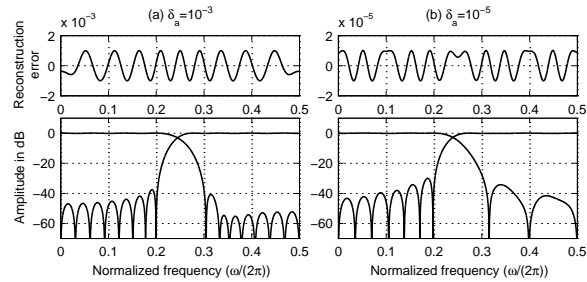


Figure 16. NPR biorthogonal filter banks with linear-phase filters.

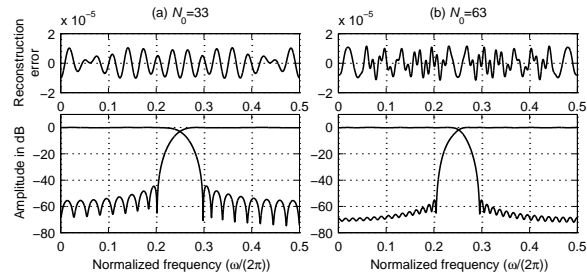


Figure 17. NPR biorthogonal filter banks with nonlinear-phase filters.

2.5 IIR Filter Banks and Their Design

This subsection reviews four alternatives for synthesizing two-channel IIR filter banks. In the first two alternatives, half-band IIR filters are used as building blocks, in the third alternative special IIR filters are used, whereas the fourth alternative uses a special structure.

2.5.1 IIR Filter Banks With Phase Distortion Generated by Using Half-Band IIR Filters

In this case, the analysis filters $H_0(z)$ and $H_1(z)$ in Figure 3 are constructed as (Wegener, 1979, Renfors, 1987)

$$H_0(z) = \frac{1}{2} [A_0(z^2) + z^{-1}A_1(z^2)] \quad (35)$$

$$H_1(z) = \frac{1}{2} [A_0(z^2) - z^{-1}A_1(z^2)], \quad (36)$$

where

$$A_0(z) = \prod_{k=1}^{K_0} \frac{a_k^{(0)} + z^{-1}}{1 + a_k^{(0)} z^{-1}} \quad (37)$$

$$A_1(z) = \prod_{k=1}^{K_1} \frac{a_k^{(1)} + z^{-1}}{1 + a_k^{(1)} z^{-1}} \quad (38)$$

are allpass filters of orders K_0 and K_1 , respectively. The orders of $H_0(z)$ and $H_1(z)$ are $2(K_0+K_1)+1$ and it is required that $K_0=K_1$ or $K_0=K_1+1$. As it can be seen $H_0(z)$ and $H_1(z)$ are related to each other through $H_1(z) = H_0(-z)$. To obtain an alias-free system the synthesis filters $F_0(z)$ and $F_1(z)$ are selected according to Equations (9) and (10), yielding

$$F_0(z) = A_0(z^2) + z^{-1}A_1(z^2) \quad (39)$$

$$F_1(z) = -A_0(z^2) + z^{-1}A_1(z^2). \quad (40)$$

In this case, the filter bank distortion function $T(z)$, as given by Equation (12), becomes

$$T(z) = z^{-1}A_0(z^2)A_1(z^2) \quad (41)$$

that is an allpass transfer function. Hence, the input-output relation suffers only from a phase distortion. This distortion is tolerable in audio applications provided that the distortion is not too large. The distortion can be reduced by adding an additional allpass filter at the end of the filter bank (Zhang and Iwakura, 1995). Figure 18 shows implementations for the overall system. The second one using the commutative models is the most efficient one (Crochiere and Rabiner, 1983).

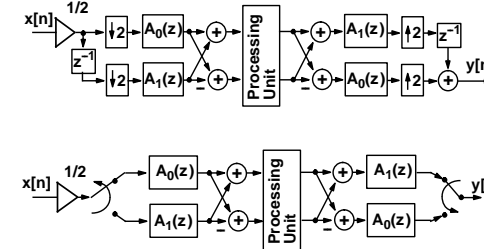


Figure 18. Efficient implementations for a two-channel filter bank based on the use of causal half-band IIR filters.

In order to compare the performance of the above IIR filter banks with the FIR banks, it is desired to design a filter bank with the stopband edge of the lowpass analysis filter being located at $\omega_s = 0.586\pi$. If the required minimum stopband attenuation is 80 dB, then the given criteria are met by $K_0=3$ and $K_1=2$. This is a special lowpass-highpass elliptic filter pair of order 11 designed by a routine written by Renfors and Saramäki (1987). The characteristics of the resulting two-channel IIR filter bank is shown in Figure 19. When comparing the amplitude responses of Figure 19 to the corresponding response of FIR filter banks considered in the previous subsection, significantly higher attenuations (80 dB) are achieved with fewer coefficients. When using wave digital filter structures with adaptor coefficients (see, e.g., Gazsi,

1985) for implementing the first-order allpass filters, only five coefficients are needed for both the analysis bank and the synthesis bank in Figure 18.

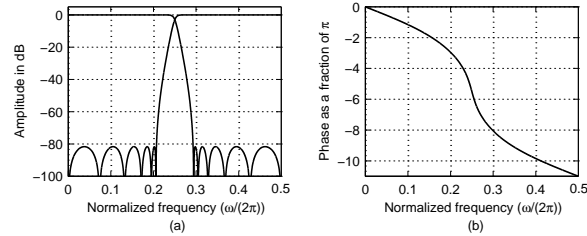


Figure 19. Two-channel IIR filter bank. (a) Amplitude responses for the analysis filters. (b) Input-output phase response for the overall filter bank.

2.5.2 PR IIR Filter Banks Using Causal and Anti-Causal Half-Band Filters

In this case, the analysis filters are constructed in the same way as in the previous subsection (Equations (35) and (36)), whereas the synthesis filters are constructed as follows:

$$F_0(z) = 2H_0(z^{-1}) = A_0(z^{-2}) + zA_1(z^{-2}) \quad (42)$$

$$F_1(z) = 2H_1(z^{-1}) = A_0(z^{-2}) - zA_1(z^{-2}) \quad (43)$$

yielding $Y(z) \equiv X(z)$ when substituting Equations (35), (36), (42), and (43) into Equations (6), (7), and (8). Figure 20 shows an implementation for the overall filter bank. The main problem in the proposed implementation is that both $F_0(z)$ and $F_1(z)$ are anti-causal filters. For finite length signals, like images, there exist several ways of implementing the filter bank using the corresponding causal filters (Ramstad, 1988; Uto, Okuda, Ikehara, and Takahashi, 1999). There exist also implementations for infinite length signals (Mitra, Creusere, and Babić, 1992). It should be pointed out that in these implementations, there is a need to produce a time-reversed version of the input data before and after filtering. This introduces an additional delay. When using the allpass filters of Figure 19 we arrive at the same amplitude responses as with the structure of Figure 18 with the exception that now there exists only a pure delay for the overall input-output response.

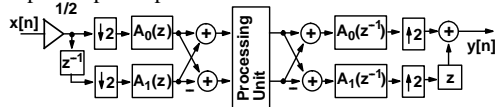


Figure 20. Implementation for a two-channel filter bank based on the use of causal and anti-causal half-band IIR filters.

2.5.3 PR IIR Filter Banks Using Special IIR Filters

The PR property is also achievable by using causal IIR filters by properly synthesizing the analysis transfer functions and relating the synthesis transfer functions to them according to Equations (9) and (10). One alternative is to construct $H_0(z)$ and $H_1(z)$ as follows:

$$H_k(z) = \frac{A_k(z)}{B_k(z^2)} = \frac{\sum_{m=0}^{M_k} a_k[m]z^{-m}}{\sum_{n=0}^{N_k} b_k[n]z^{-2n}} \quad \text{for } k = 0, 1. \quad (44)$$

In this case, $T(z)$, as given by Equation (12), becomes

$$T(z) = \frac{A_0(z)A_1(-z) - A_0(-z)A_1(z)}{B_0(z^2)B_1(z^2)} \quad (45)$$

and the PR property implies that $T(z) = z^{-K}$ with K being an odd integer.

Filter banks of this type have been originally proposed by Basu, Chiang, and Choi (1995) but no practical design methods have been given. Afterwards, optimization (Mao, Chan, and Ho, 1999) and some transformation approaches (Tay, 1998) have been introduced for synthesizing these filter banks.

Due to the use of IIR filters, the desired channel selectivity compared to FIR filter banks can be achieved using fewer coefficients. As an example, consider the design of a filter bank with $M_0 = M_1 = 21$, $N_0 = N_1 = 2$, $K = 19$, and the passband and stopband edges being located at 0.414π and 0.586π , like in the previous examples. The maximum allowable passband ripple is 0.01 and the maximum amplitude value in the transition bands is 1.01. The use of constrained optimization minimizing the maximum of the stopband energies of the analysis filters subject to the given constraints results in the responses shown in Figure 21 (Bregović and Saramäki 2001b).

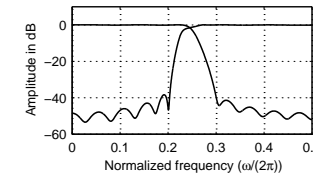


Figure 21. IIR filter bank using special IIR filters.

2.5.4 PR IIR Filter Banks Based on a Special Structure

Another alternative to generate a PR filter bank using causal IIR filters is to construct the analysis and synthesis filters as shown in Figure 22. This structure has been introduced by Kim and Ansari (1991) and later modified by Phoong, Kim, and Vaidyanthan (1995).

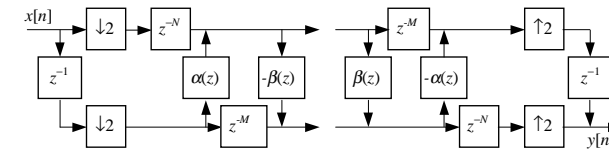


Figure 22. Special structure for two-channel IIR filter banks.

For this structure, the analysis filter transfer functions are constructed as follows:

$$H_0(z) = \frac{1}{2} [z^{-2N} + z^{-1}\alpha(z^2)] \quad (46)$$

$$H_1(z) = -\beta(z^2)H_0(z) + z^{-2M-1}, \quad (47)$$

whereas the synthesis filter transfer functions are related to these functions according to Equations (9) and (10). The above transfer functions are constructed such that $T(z)$, as given by Equation (12), is $z^{-2N-2M-1}$ independent of the selection of the transfer functions $\alpha(z)$ and $\beta(z)$. Therefore, the design of the PR filter bank can concentrate only on generating good frequency responses for $H_0(z)$ and $H_1(z)$. Hence, for causal filter banks, $\alpha(z)$ and $\beta(z)$ can be selected to be any causal IIR or FIR filter transfer functions.

Two basic approaches have been proposed for selecting $\alpha(z)$ and $\beta(z)$. In the first approach, $\alpha(z) \equiv \beta(z)$ and $M = 2N - 1$ (Phoong, Kim, and Vaidyanathan, 1995) with $\beta(z)$ being an allpass transfer function of order N or $N - 1$ or a linear-phase FIR transfer function of order $2N - 1$ having a symmetrical impulse response. In both cases, there is always a bump in the amplitude response of $H_1(z)$ in the transition band of approximately 4 dB. In the second approach, $\alpha(z)$ and $\beta(z)$ are different transfer functions. In this case, $\alpha(z)$ and $\beta(z)$ are a causal allpass filter transfer function and a linear-phase FIR filter function with symmetrical impulse response, respectively (Chan, Mao, and Ho, 2000). They can also be selected to be nonlinear-phase FIR filter transfer functions (Mao, Chan, and Ho, 2000). In addition to the structure depicted in Figure 22, a slightly modified structure has been proposed by Zhang and Yoshikawa in (1998, 1999).

3 Multi-Channel (M-Channel) Filter Banks

There exist three basic approaches for designing multi-channel uniform filter bank. In the first technique, all the analysis and synthesis filters are considered to be independent and they are optimized simultaneously to meet the PR or NPR property. For the PR case see, e.g., Vaidyanathan et al. (1989). The second approach is based on building the filter bank using a tree-structure with two-channel filter banks as building blocks. In the third technique, a single prototype filter is synthesized and the overall bank is generated with the aid of a cosine-modulation or a modified discrete Fourier transform (MDFT) technique. This section concentrates on the last two approaches.

3.1 Tree-Structured Filter Banks Using Two-Channel Filter Banks as Building Blocks

When generating a tree-structured filter bank, a two-channel filter bank as shown in Figure 23(a) is used as a starting point. For this bank, the analysis and synthesis filters are denoted by $H_0^{(1)}(z)$, $H_1^{(1)}(z)$, $F_0^{(1)}(z)$, and $F_1^{(1)}(z)$. The next step is to remove the processing unit in Figure 23(a) and produce $y_0^{(1)}[n]$ $\{y_1^{(1)}[n]\}$ from $x_0^{(1)}[n]$ $\{x_1^{(1)}[n]\}$ using a two-channel filter bank shown in Figure 23(b). For this bank, the analysis and synthesis filters are denoted by $H_0^{(2)}(z)$, $H_1^{(2)}(z)$, $F_0^{(2)}(z)$, and $F_1^{(2)}(z)$. This results in the two-level, tree-structured filter bank shown in Figure 23(c).

The three-level tree-structured filter bank shown in Figure 24 is obtained by removing the processing unit in Figure 23(c) and producing $y_k^{(2)}[n]$ from $x_k^{(2)}[n]$ for $k = 0, 1, 2, 3$ using a two-channel filter bank with the analysis and synthesis filters being $H_0^{(3)}(z)$, $H_1^{(3)}(z)$, $F_0^{(3)}(z)$, and $F_1^{(3)}(z)$. In order to analyze the performance of the three-level tree-structured filter bank of

Figure 24, it can be redrawn as the equivalent form also shown in Figure 24. Hence, it corresponds to a uniform analysis-synthesis bank with 8 channels. Four-level tree-structured filter banks can be generated by removing the processing unit and producing $w_k^{(3)}[n]$ from $v_k^{(3)}[n]$ for $k = 0, 1, \dots, 7$ using a two-channel filter bank. In this case, the number of channels is 16. In general, for a K -level tree-structured filter bank, the number of channels is 2^K .

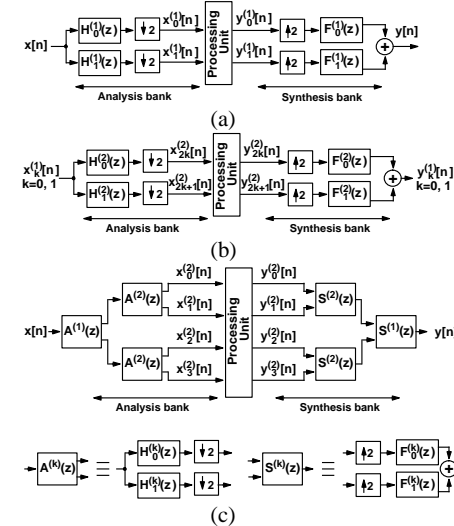


Figure 23. Generation of a two-level tree-structured filter bank.

Next an example will be given illustrating how to select the building-block two-channel filter banks. It is desired to generate an analysis-synthesis filter bank with 8 channels by using a three-level tree-structured filter bank. The required transition bandwidth and the attenuation are 0.05π and 60 dB, respectively. As two-channel filter banks, causal half-band IIR filters considered in Subsection 2.5.1 are used. For all the banks, the required attenuation is 60 dB, whereas the required stopband edges are located at 0.525π , 0.55π , and 0.6π for the first, second, and third two-channel banks, respectively. The given criteria are met by $K_0 = K_1 = 3$; $K_0 = 3$ and $K_1 = 2$; and $K_0 = K_1 = 2$; respectively. It should be pointed out that when using a tree-structured filter bank in general, the transition bandwidth for the first building block is the specified one, whereas for the k th block, it is 2^{k-1} times that of the specified one. This is basically due to the equivalent structure of Figure 24, where, instead of a unit delay, a block of 2^{k-1} delay elements is used. For the influence of this fact, see, e.g., Saramäki (1993).

The amplitude responses of the three two-channel filter banks as well as the amplitude responses between the input $x[n]$ and $v_k[n]$ for $k = 0, 1, \dots, 7$ (see Figure 24) are depicted in Figure 25. The numbers in the figure indicate the corresponding responses. The responses between $w_k[n]$ for $k = 0, 1, \dots, 7$ and the output $y[n]$ are the same with the exception that they are obtained by multiplying the responses of Figure 25(b) by eight.

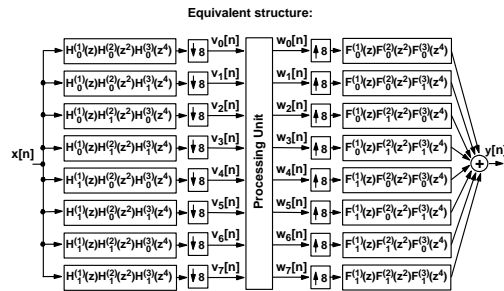
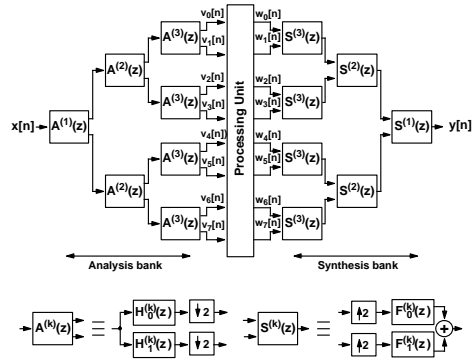


Figure 24. Three-level tree-structured filter bank.

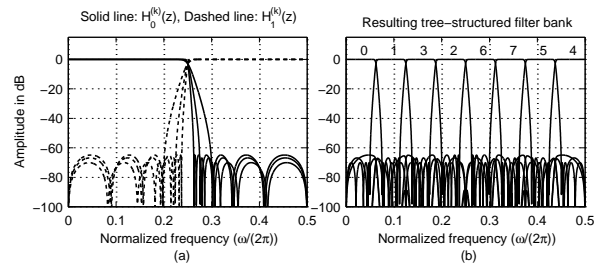


Figure 25. Three-level tree-structured filter bank. (a) Amplitude responses for the analysis filters in the three building blocks. Filters with the narrowest, the second narrowest, and the widest transition band correspond to the first, second, and third building blocks, respectively, that is, for $H_0^{(k)}(z)$ and $H_1^{(k)}(z)$ for $k=0,1,3$. (b) Amplitude responses for the resulting filters between the input $x[n]$ and $v_k[n]$ for $k=0,1,\dots,7$ in Figure 24. The numbers in the figure indicate the corresponding responses.

3.2 Cosine-Modulated Filter Banks

Among different classes of M -channel critically sampled filter banks, cosine-modulated and MDFT filter banks have become very popular in many applications due to the following reasons. First, both the analysis and synthesis filters for these banks can be generated using one or two prototype filters by exploiting proper transformations, making the overall implementation effective. Second, the overall synthesis can concentrate on optimizing only the prototype filter(s). This subsection considers the design and properties of PR and NPR cosine-modulated filter banks. The properties of MDFT banks will then be discussed in Subsection 3.3. As has been pointed out by Karp and Fliege (1999) and Heller, Karp, and Nguyen (1999), the same prototype filter with a proper scaling can be used for both filter bank types mentioned above.

One of the first observations on how to generate NPR M -channel critically sampled filter banks with the aid of a single prototype filter and a proper cosine modulation was made by Rothweiler (1983). Since then, intensive research has been performed for designing and implementing PR and NPR cosine-modulated filter banks. Historically, the first cosine-modulated filter banks were generated from a single linear-phase prototype filter in such a way that the impulse responses of the corresponding analysis and synthesis filters were flipped versions of each other (Malvar, 1990, 1991, 1992a, 1992b; Ramstad and Tanem, 1991; Koilpillai and Vaidyanathan, 1991, 1992; Saramäki, 1992; Nguyen, 1992b, 1994, 1995; Vaidyanathan, 1993; Creusere and Mitra 1995; Nguyen and Koilpillai, 1996; Mertins, 1998; Saramäki and Bregović, 2001; Bregović and Saramäki, 2001a). Later on, these filter banks are referred to as orthogonal cosine-modulated banks. In this case, the filter bank delay is equal to the order of the prototype filter. More recently, new synthesis schemes have been proposed for synthesizing cosine-modulated filter banks where the filter bank delay is lower than the order of the prototype filter (Nguyen, 1992a; Xu et al., 1996; Schuller, 1997; Karp and Mertins, 1997; Goh and Lim, 1999b; Heller, Karp, and Nguyen, 1999; Argenti and Del Re, 2000; Schuller and Karp, 2000; Karp, Mertins, and Schuller, 2001). For these banks the prototype filter for generating the analysis and synthesis filters may be different. These filter banks are referred to as low-delay biorthogonal cosine-modulated filter banks.

3.2.1 Input-output relations for M -channel critically sampled filter banks

A general M -channel critically sampled filter bank is shown in Figure 1(a). For this system, the input-output relation in the z -domain is expressible as

$$Y(z) = T_0(z)X(z) + \sum_{l=1}^{M-1} T_l(z)X(z e^{-j2\pi l/M}), \quad (48)$$

where

$$T_0(z) = \frac{1}{M} \sum_{k=0}^{M-1} F_k(z)H_k(z) \quad (49)$$

and

$$T_l(z) = \frac{1}{M} \sum_{k=0}^{M-1} F_k(z)H_k(z e^{-j2\pi l/M}) \quad \text{for } l=1, 2, \dots, M-1. \quad (50)$$

Here, $T_0(z)$ is called the distortion transfer function and determines the distortion caused by the overall system for the unaliased component $X(z)$ of the input signal. The remaining transfer functions $T_l(z)$ for $l=1, 2, \dots, M-1$ are called the alias transfer functions and determine how well the aliased components $X(z e^{-j2\pi l/M})$ of the input signal are attenuated.

For the PR property, it is required that $T_0(z) = z^{-K}$ with K being an integer and $T_l(z) = 0$ for $l = 1, 2, \dots, M-1$. If these conditions are satisfied, then the output signal is a delayed version of the input signal, that is, $y[n] = x[n-K]$. It should be noted that PR is exactly achieved only in the case of lossless coding. For a lossy coding, PR is not achieved. Therefore, amplitude and aliasing errors being less than those caused by coding are allowed. In these NPR cases, the above-mentioned conditions should be satisfied within given tolerances.

3.2.2 PR and NPR cosine-modulated filter banks

The impulse responses of the analysis and synthesis transfer functions $H_k(z)$ and $F_k(z)$ for $k = 0, 1, \dots, M-1$ for PR and NPR M -channel critically-sampled cosine-modulated filter banks as shown in Figure 1(a) can be generated with the aid of an FIR prototype filter with the following transfer function:

$$H_p(z) = \sum_{n=0}^N h_p[n] z^{-n} \quad (51)$$

as

$$h_k[n] = 2h_p[n] \cos\left(\frac{\pi}{M} \left(k + \frac{1}{2}\right) \left(n - \frac{K}{2}\right) + (-1)^k \pi/4\right) \quad (52)$$

$$f_k[n] = 2h_p[n] \cos\left(\frac{\pi}{M} \left(k + \frac{1}{2}\right) \left(n - \frac{K}{2}\right) - (-1)^k \pi/4\right). \quad (53)$$

for $n = 0, 1, \dots, N$.

It should be pointed out that in the most general case, the prototype filters for generating the analysis and synthesis filters could be different (Heller et al., 1999; Karp et al., 2001). However, without loss of generality, they can be selected to be equal in most practical cases. In the above equations, K is the filter bank delay and is usually expressed as $K = 2sM + d$ where s is an integer larger than or equal to zero and $0 \leq d < 2M$. In general, K can be chosen arbitrarily in the range $K \in [M-1, 2N-M+3]$. However, in order to obtain a low-delay biorthogonal filter bank, K must be less than the prototype filter order N ($K < N$). In the case of orthogonal cosine-modulated filter banks, $K = N$ and the impulse response of the prototype filter $H_p(z)$ has an even symmetry, that is, $h_p[N-n] = h_p[n]$ for $n = 0, 1, \dots, N$. Furthermore, $f_k[n] = h_k[N-n]$ for $k = 0, 1, \dots, M-1$ and for $n = 0, 1, \dots, N$.

It should be pointed out that because of interpolation by a factor of M , the amplitude responses of both the analysis and synthesis filters resulting when using the design schemes, to be described later on in this chapter, approximate \sqrt{M} in their passbands. This means that if the peak scaling for the fixed-point arithmetic is desired to be used, the analysis (synthesis) filters should be divided (multiplied) by this constant. In the sequel, when giving the amplitude responses of the prototype filter as well as those of the analysis and synthesis filters they are normalized to approximate unity in the passbands.

The key idea of designing the prototype filter and using the above-mentioned modulation scheme is based on the following facts. First, the prototype filter is designed in such a manner that its amplitude response $|H_p(e^{j\omega})|$ achieves approximately the value of 1/2 at $\omega = \pm\pi(2M)$ and the stopband edges are located at $\omega = \pm\omega_s$ with $\omega_s = \pi(1+\rho)/(2M)$, $\rho > 0$ as shown in Figure 26(a) in the $M = 4$ case. Then, due to the cosine-modulation, the amplitude responses of the analysis filters are given by $|H_k(e^{j\omega})| = |H_p(e^{j(\omega - (2k+1)\pi/(2M))})| + |H_p(e^{j(\omega + (2k+1)\pi/(2M))})|$ as shown in Figure

26(b). Hence, for the k th analysis filter, the amplitude response is obtained by shifting that of the prototype filter to the left and right in the frequency axis by $\omega_k = (2k+1)\pi/(2M)$. Therefore, for the k th bandpass analysis filter with transfer function $H_k(z)$ with $1 \leq k \leq M-2$, the passband center is located at $\omega = \omega_k$ and the stopband edges at $\omega = \omega_k \pm \omega_s$. For the lowpass filter with transfer function $H_0(z)$, the value of unity is approximately achieved at $\omega = 0$ since both shifted versions achieve the value of 1/2 at this angular frequency and the stopband edge is located at $\omega = \pi/(2M) + \omega_s = \pi(2+\rho)/(2M)$. This is approximately true for the orthogonal filter banks, but not for low-delay biorthogonal filter banks, as will be seen in connection with examples. Similarly, for the highpass filter $H_{M-1}(z)$, the value of unity is approximately achieved at $\omega = \pi$ and the stopband edge is located at $\omega = \pi - \pi(2+\rho)/(2M)$.

Second, the above-mentioned cosine-modulation technique has the attractive property that if the prototype filter is designed in the proper manner, then the overall uniform filter bank will achieve the PR property. This is based on the fact that the aliasing components generated in the analysis bank are compensated in the synthesis bank, like explained earlier in the case of two-channel filter banks (see Subsection 2.1 and 2.2).

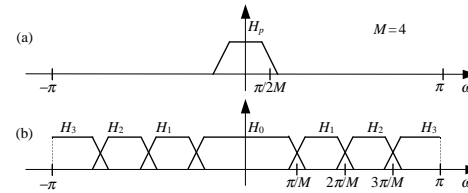


Figure 26. Frequency responses of a four-channel cosine-modulated filter bank. (a) Prototype filter. (b) Analysis filters.

3.2.3 PR cosine-modulated filter banks and their implementation

The criteria for the PR property can be conveniently stated by decomposing the prototype filter transfer function, as given by Eq. (51), into $2M$ polyphase components (Malvar, 1992a, Vaidyanathan, 1993) as follows:

$$H_p(z) = \sum_{l=0}^{2M-1} z^{-l} G_l(z^{2M}), \quad g_l[m] = h_p[2mM + l]. \quad (54)$$

There are the following two cases of interest depending on the value of d in $K = 2sM + d$ (Heller et al., 1999; Karp et al., 2001):

1) PR constraints for $0 \leq d < M$:

$$G_l(z)G_{d-l}(z) + z^{-1}G_{M+l}(z)G_{M+d-l}(z) = \frac{z^{-s}}{2M}, \quad 0 \leq l \leq d,$$

$$G_l(z)G_{2M+d-l}(z) + G_{M+l}(z)G_{M+d-l}(z) = \frac{z^{-(s-1)}}{2M}, \quad d < l < 2M, l \neq \frac{M+d}{2},$$

$$G_l(z)G_{l+M}(z) = \begin{cases} z^{-(s-1)}/(4M) & \text{for } s \text{ odd} \\ -z^{-(s-1)}/(4M) & \text{for } s \text{ even,} \end{cases} \quad \text{if } l = \frac{M+d}{2} \text{ is an integer.}$$

2) PR constraints for $M \leq d < 2M$:

$$G_l(z)G_{d-l}(z) + G_{M+l}(z)G_{d-l-M}(z) = \frac{z^{-s}}{2M}, \quad 0 \leq l \leq d-M, l \neq \frac{d-M}{2},$$

$$G_l(z)G_{d-l}(z) + z^{-1}G_{l+M}(z)G_{M+d-l}(z) = \frac{z^{-s}}{2M}, \quad d-M < l < 2M,$$

$$G_l(z)G_{l+M}(z) = \begin{cases} -z^{-s}/(4M) & \text{for } s \text{ odd} \\ z^{-s}/(4M) & \text{for } s \text{ even,} \end{cases} \quad \text{if } l = \frac{d-M}{2} \text{ is an integer.}$$

These conditions can be directly exploited in optimizing the prototype filters for simultaneously achieving the PR property and generating filter banks with high frequency selectivities. Furthermore, the above polyphase decomposition can be utilized in developing efficient realizations for the overall filter bank. One alternative realization form is shown in Figure 27 with the elements of the cosine-transform matrices given by Heller et al. (1999) and Karp et al. (2001)

$$[\mathbf{C}_1]_{kl} = 2\cos\left(\frac{\pi}{M}\left(k + \frac{1}{2}\right)\left(l - \frac{K}{2}\right) + (-1)^k \pi/4\right) \quad (55)$$

$$[\mathbf{C}_2]_{kl} = 2\cos\left(\frac{\pi}{M}\left(k + \frac{1}{2}\right)\left(2M - 1 - l - \frac{K}{2}\right) - (-1)^k \pi/4\right) \quad (56)$$

for $0 \leq k < M$ and $0 \leq l < 2M$. In this figure, the left side generates, with the aid of the polyphase components and the $M \times 2M$ transform matrix \mathbf{C}_1 , the analysis bank with M decimated sub-signals that are used as inputs to the processing unit of Figure 1(a). Similarly, the right side of Figure 27 forms the synthesis bank of Figure 1(a). The actual $2M \times M$ transform matrix \mathbf{C}_2^T is the transpose of the $M \times 2M$ matrix \mathbf{C}_2 . After some rearrangements, the above transforms can be implemented effectively using a Type III or a Type IV discrete cosine transform (a DCT-III or a DCT-IV) (Vaidyanathan 1993; Heller et al., 1999; Karp et al., 2001) depending on whether the overall filter bank delay K is even or odd, respectively. As shown in Karp et al. (2001), in the structure of Figure 27 the transform matrices can be reduced to be of size $M \times M$ after some modifications.

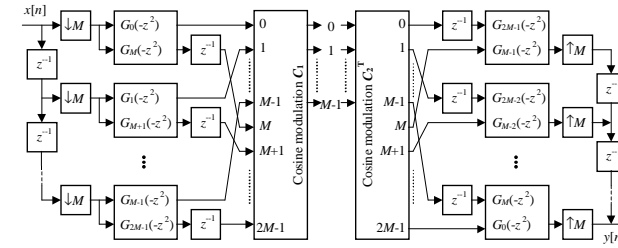


Figure 27. Realization of the analysis and synthesis filters for the cosine-modulated filter bank with the aid of the polyphase components of the prototype filter and transform matrices \mathbf{C}_1 and \mathbf{C}_2^T .

There exist two alternatives for generating the component pairs $G_l(-z^2)$ and $G_{l+M}(-z^2)$ of the analysis and synthesis filters for $l=0, 1, \dots, M-1$ in the biorthogonal case. The simplest way to implement the polyphase components $G_l(-z^2)$ for $l=0, 1, \dots, 2M-1$ is to use direct-form realizations. Computationally more efficient realizations have been developed by Schuller (1997), Karp and Mertins (1997), Schuller and Karp (2000), and Karp, Mertins, and Schuller (2001). Among them, the realization introduced by Karp, Mertins, and Schuller (2001) is the most general (can be used for any values of N and K) and computationally the most efficient. Compared to the direct-form implementations of the polyphase components, the number of multipliers and adders required by their structure is approximately halved. An attractive feature of this structure is that the PR condition is preserved independent of the coefficient values, thereby enabling us to express them in very simple representation forms. For the orthogonal case ($K=N$), the component pairs $G_l(-z^2)$ and $G_{l+M}(-z^2)$ for $l=0, 1, \dots, M-1$ can be implemented simultaneously using two-channel lossless lattice structures (Koipillai and Vaidyanathan, 1992; Vaidyanathan, 1993; Nguyen and Koipillai, 1996). A computationally very efficient realization has been developed by Malvar in (Malvar 1992a, 1992b) in the case where $N=K=2LM-1$ with L being an integer. It is based on the use of special butterflies and the DCT-IV. This has been achieved by using a slightly different cosine-modulation technique.

It should be pointed out that in the NPR orthogonal and low-delay biorthogonal cases, the only alternative to implement the polyphase components $G_l(-z^2)$ for $l=0, 1, \dots, 2M-1$ is to use direct-form realizations. Also, in the case of Malvar's structure (Malvar 1992a, 1992b), the butterflies cannot be used and there is a need to modify the structure.

3.2.4 Orthogonal and biorthogonal cosine-modulated filter banks under consideration

In theory, the PR orthogonal (PR low-delay biorthogonal) cosine-modulated filter bank can be optimized for any values of M and $N=K$ (any values of M , N , and K). However, it has turned out that the best filter bank performances are achieved by selecting these integers such that there are no constraints on the impulse-response coefficients of the prototype filter. These selections result in filter banks with highest channel selectivities and highest attenuations. The other choices may give rise to filters with a lower filter bank delay and lower orders for the analysis and synthesis filters. The price to be paid for the additional constraints on the impulse-response coefficients of the prototype filter (some coefficient values are restricted to take on the predetermined values or they are restricted to be zero-valued) is that the resulting filter performances are worse than for the cases without constraints. This section concentrates on the following two cases:

1. Orthogonal banks with arbitrary M and $N=K=2LM-1$ with L being an integer.
2. Biorthogonal banks with even M , $N=2LM-1$ with L being an integer, and $d=2M-1$, that is, $K=2sM+d=2(s+1)M-1$.

It has been observed by Koilpillai and Vaidyanathan (1992) that it is straightforward to design orthogonal filter banks with an odd number of channels and a good overall performance, even though there are constraints on the impulse-response coefficients of the prototype filter. More research work should be done to find out whether the same is true for low-delay biorthogonal filter banks.

3.2.5 Statement of the optimization problem for PR and NPR cosine-modulated filter banks

The optimization problem can be stated for both PR and NPR filter banks in the following two ways:

Least-Squares Optimization Problem: Given $\omega_s = (1 + \rho)\pi/(2M)$, M , and N as well as K for the low-delay biorthogonal case, find the coefficients of the prototype filter transfer function $H_p(z)$, as given by Equation (51) to minimize

$$E_2 = \int_{\omega_s}^{\pi} |H_p(e^{j\omega})|^2 d\omega, \quad (57)$$

subject to

$$|T_0(e^{j\omega}) - e^{-j\omega K}| \leq \delta_1 \quad \text{for } \omega \in [0, \pi] \quad (58)$$

and

$$|T_l(e^{j\omega})| \leq \delta_2 \quad \text{for } \omega \in [0, \pi] \quad (59)$$

for $l = 1, 2, \dots, M-1$.

Minimax Optimization Problem: Given $\omega_s = (1 + \rho)\pi/(2M)$, M , and N as well as K for the low-delay biorthogonal case, find the coefficients of $H_p(z)$ to minimize

$$E_\infty = \max_{\omega \in [\omega_s, \pi]} |H_p(e^{j\omega})| \quad (60)$$

subject to the conditions of Equations (58) and (59).

In these optimization problems, the main goal is to minimize the stopband response of the prototype filter either in the least-mean-square sense or in the minimax sense subject to two constraints. First, the maximum of the absolute value of the deviation between the overall frequency response for the unaliased term and the delay of K samples should be in the baseband less than or equal to δ_1 . Second, the maximum value of the worst-case aliasing term should be less than or equal to δ_2 . For the NPR orthogonal case, the phase response of $T_0(z)$ is linear ($-K\omega$) and δ_1 is directly the maximum deviation of the amplitude response from unity. For the NPR low-delay biorthogonal case, $T_0(z)$ suffers from both phase and amplitude distortions.

3.2.6 Design of PR and NPR orthogonal and biorthogonal cosine-modulated filter banks

For the PR case, it is required that $\delta_1 = \delta_2 = 0$. Optimizing the prototype filter in such a manner that the overall filter bank becomes PR is a nonlinear problem. To solve this problem conveniently in the orthogonal case where $N=K=2LM-1$ with L being an integer, the angles for the lattice structures in the prototype filter for PR cosine-modulated filter banks (Koilpillai et al., 1992, Malvar, 1992a) can be used as unknowns. In this case, the PR property is achieved

independent of the angle values. Simultaneously, the original constrained optimization problem becomes unconstrained and the number of unknowns reduces to $L \lfloor M/2 \rfloor$ ($\lfloor x \rfloor$ stands for the integer part of x). Despite of this simplification, there exist several local optima when minimizing the stopband response of the prototype filter in the minimax or in the least-mean-square sense. To alleviate this problem Saramäki (1992, 1998) and Bregović, and Saramäki (2001a) have proposed systematic multi-step approaches to arrive at least at a good local optimum for large values of M and L .

For the PR biorthogonal case, there exist two principal approaches to arrive at a good local optimum. Similarly to the orthogonal case mentioned above, Schuller and Smith (1996), Schuller (1997), Schuller and Karp (2000), and Karp et al. (2001) have developed a technique where the actual design can concentrate on optimizing the proper parameters, uniquely specifying the filter bank performance, in such a way that the PR property is guaranteed independent of their values. Hence, the overall optimization problem becomes unconstrained. In the second approach, Nguyen (1992b, 1995) and Heller et al. (1999) use constrained least-squares optimization. In this technique, the stopband energy of the prototype filter is optimized subject the PR constraints mentioned in Subsection 3.2.3.

For synthesizing NPR orthogonal filter banks, an efficient two-step procedure has been described by Saramäki and Bregović (2001). In the first step, a good start-up solution is generated with the aid of a prototype filter for the PR case. In the second step, nonlinear optimization is applied for further optimizing the prototype filter subject to the given constraints. A similar technique has also been applied for designing NPR low-delay biorthogonal filter banks by Bregović and Saramäki (2001c). In addition to the above-mentioned design methods, an iterative technique has been proposed by Xu et al. (1996) for designing NPR orthogonal and low-delay biorthogonal filter banks. This design scheme gives very fast suboptimal filter banks. In addition, it allows us to control the artifacts of low-delay biorthogonal banks to be considered in connection with examples.

3.2.7 Comparison between PR and NPR cosine-modulated filter banks

For comparison purposes, several orthogonal filter banks have been optimized for $M=32$ channels and $\rho=1$, that is, the stopband edge of the prototype filter is located at $\omega_s = \pi/32$. The results are summarized in Table III. In all cases under consideration, the order of the prototype filter is $N=2LM-1$, where L is an integer and the stopband response has been optimized in either the minimax or least-mean-square (LSQ) sense. δ_1 shows the maximum deviation of the amplitude response of the distortion transfer function $T_0(z)$ from unity, whereas δ_2 is the maximum amplitude value of the worst-case aliasing transfer function $T_l(z)$. The boldface numbers indicate those parameters that have been fixed in the optimization. E_∞ and E_2 give the maximum stopband amplitude value of the prototype filter and its stopband energy, respectively.

Designs 1 and 2 in Table III are PR filter banks, whereas designs 4, 5, and 6 have been optimized subject to the given amplitude error for $T_0(z)$ without taking into account the aliasing errors. For designs 7 and 8, the optimization has been performed subject to the given amplitude and aliasing errors.

Table III Comparison between orthogonal filter banks with $M=32$ and $\rho=1$. Boldface numbers indicate those parameters that have been fixed in the optimization.

Design	Criterion	N	δ_1	δ_2	E_∞	E_2
1	LSQ	511	0	0 ($-\infty$ dB)	$1.2 \cdot 10^{-3}$ (-58 dB)	$7.4 \cdot 10^{-9}$
2	Minimax	511	0	0 ($-\infty$ dB)	$2.3 \cdot 10^{-4}$ (-73 dB)	$7.5 \cdot 10^{-8}$
3	LSQ	511	10^{-4}	$2.3 \cdot 10^{-6}$ (-113 dB)	$1.0 \cdot 10^{-3}$ (-100 dB)	$5.6 \cdot 10^{-13}$
4	Minimax	511	10^{-4}	$1.1 \cdot 10^{-5}$ (-99 dB)	$5.1 \cdot 10^{-6}$ (-106 dB)	$3.8 \cdot 10^{-11}$
5	LSQ	511	0	$9.1 \cdot 10^{-5}$ (-81 dB)	$4.5 \cdot 10^{-4}$ (-67 dB)	$5.4 \cdot 10^{-10}$
6	LSQ	511	10^{-2}	$5.3 \cdot 10^{-7}$ (-126 dB)	$2.4 \cdot 10^{-9}$ (-112 dB)	$4.5 \cdot 10^{-14}$
7	LSQ	383	10^{-3}	10^{-5} (-100 dB)	$1.7 \cdot 10^{-4}$ (-75 dB)	$8.8 \cdot 10^{-10}$
8	LSQ	319	10^{-2}	10^{-4} (-80 dB)	$8.4 \cdot 10^{-4}$ (-62 dB)	$2.7 \cdot 10^{-9}$

Some characteristics of designs 1 and 3 are depicted in Figure 28(a) and Figures 28(b) and 28(c), respectively. From these figures as well as from Table III, it is seen that the NPR filter banks provide significantly improved filter bank performances at the expense of a small amplitude error and very small aliasing errors. When comparing designs 2 and 4 in Table III, it is seen that the same is true for the corresponding minimax designs.

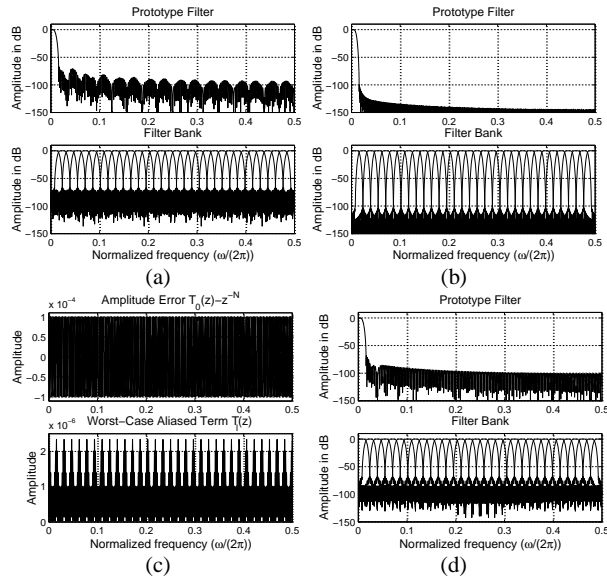


Figure 28. Characteristics of PR and NPR cosine-modulated orthogonal filter banks of $M=32$ filters for $\rho=1$ designed in the least-mean-square sense. (a) PR filter bank with filter orders $N=511$ (design 1 in Table III). (b) and (c) NPR filter bank with filter orders $N=511$ designed subject to the constraint $\delta_1=0.0001$ (design 3 in Table III). (d) NPR filter bank with filter orders $N=319$ designed subject to the constraints $\delta_1=0.01$ and $\delta_2=0.0001$ (design 6 in Table III).

When comparing designs 1 and 5 in Table III, it is observed that even an optimized NPR filter bank without any amplitude error for $T_0(z)$ (also considered in Nguyen, 1994) provides a considerably better performance than the PR filter bank. Furthermore, it is seen that the performance of the NPR filter bank significantly improves when a higher amplitude error is allowed (design 6 in Table III). Some of the characteristics of design 8 are depicted Figure 28(d). When comparing this solution with design 1 of Table III (see also Figure 28(a)), it is observed that the same or even a better filter bank performance can be achieved with a significantly lower filter order (319 compared with 511) when small amplitude and aliasing errors are allowed.

Table IV compares PR orthogonal, PR low-delay biorthogonal, and NPR low-delay biorthogonal cosine-modulated filter banks for $M=32$ channels and $\rho=1$, like in the case of Table III. Designs 1, and 4 are PR orthogonal banks and designs 2 and 5 PR low-delay biorthogonal filter banks, whereas designs 3 and 6 are NPR low-delay biorthogonal banks. Some characteristics of designs 3 are depicted in Figure 29. Several interesting observations can be made based on the results of Table IV. When comparing designs 1 and 2, it is seen that design 2 provides a significant improvement in the selectivity by increasing the prototype filter order by approximately 50 %. Similarly, design 5 provides a considerable improvement compared to design 4 by increasing the prototype filter order by approximately 100 %. For the NPR low-delay designs 3 and 6, the performances of the prototype filters are significantly better than for the corresponding PR designs (designs 2 and 5) at the expense of a small error for $T_0(z)$ and small aliasing errors. For design 3 (design 6), the group delay response for the unaliased component approximates 255 with tolerance equal to 0.31 (191 with tolerance equal to 2.4).

Its very interesting to observe that the prototype filters for the NPR designs 3 and 6 are slightly better than that for design 1 of Table III. It should be noted that for design 3 of Table IV (design 6 of Table IV), the prototype filter order and the filter bank delay are only approximately 75 % (75 %) and 50 % (37 %) compared to those of design 1 of Table III.

Table IV Comparison between PR orthogonal, PR low-delay biorthogonal, and NPR low-delay biorthogonal cosine-modulated filter banks with $M=32$ and $\rho=1$. Boldface numbers indicate those parameters that have been fixed in the optimization.

Design	N	K	δ_1	δ_2	E_∞	E_2
1	255	255	0	0 ($-\infty$ dB)	$2.3 \cdot 10^{-2}$ (-33 dB)	$4.2 \cdot 10^{-6}$
2	383	255	0	0 ($-\infty$ dB)	$8.3 \cdot 10^{-3}$ (-41 dB)	$5.2 \cdot 10^{-7}$
3	383	255	0.001	10^{-5} (-100 dB)	$1.1 \cdot 10^{-3}$ (-59 dB)	$2.7 \cdot 10^{-9}$
4	191	191	0	0 ($-\infty$ dB)	$4.2 \cdot 10^{-2}$ (-28 dB)	$2.9 \cdot 10^{-5}$
5	383	191	0	0 ($-\infty$ dB)	$8.4 \cdot 10^{-3}$ (-41 dB)	$6.2 \cdot 10^{-7}$
6	383	191	0.01	10^{-4} (-80 dB)	$1.3 \cdot 10^{-3}$ (-58 dB)	$4.2 \cdot 10^{-9}$

Compared to orthogonal cosine-modulated filter banks, the improvements provided by low-delay biorthogonal filter banks cannot be achieved without artifacts, as has been pointed out by Xu et al. (1996). First, the amplitude response of the (normalized) prototype filter achieves an overshoot in the transition band. Second, the amplitude response of the (normalized) lowpass (highpass) analysis filter does not achieve the value of unity at $\omega=0$ ($\omega=\pi$). For instance, for the prototype filter of Figure 29, the maximum amplitude value in the transition band is 0.62 dB, whereas the lowpass (highpass) analysis filter achieves the value of -5.1 dB at $\omega=0$ (5.1 dB at $\omega=\pi$). As shown by Xu et al. (1996) and Karp et al. (2001), these artifacts can be reduced at the

expense of lower attenuations for the analysis and synthesis filters by imposing extra constraints in the filter bank design.

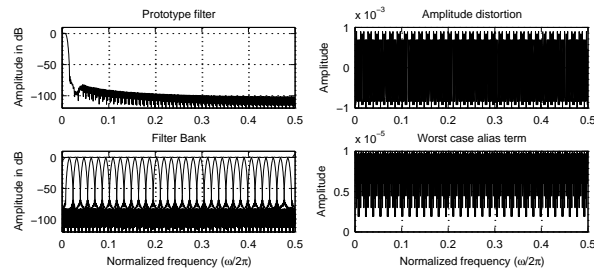


Figure 29. Characteristics of NPR low-delay biorthogonal filter bank of $M=32$ filters for $\rho=1$ designed in the least-mean-square sense. $\delta_1=0.001$ and $\delta_2=10^{-5}$ (design 3 in Table IV).

3.3 Modified DFT Filter Banks

For implementing an M -channel (M is even) MDFT filter bank, a prototype filter for an $M/2$ -channel cosine-modulated filter bank can be used directly in both PR and NPR cases after scaling it by a factor of $\sqrt{2}$ (Karp and Fliege, 1999). Therefore, this subsection concentrates mainly on the properties of MDFT filter banks and their relations to cosine-modulated filter banks. First, these banks are developed for a complex-valued input signal. After that, it is shown how this bank can be simplified for a real-valued input data.

3.3.1 MDFT filter banks for complex-valued input data

In the original MDFT filter banks introduced by Fliege (1993) and Karp and Fliege (1999) it is assumed that both the input and output signals for the filter bank as shown in Figure 1(a) are complex-valued. Furthermore, M is restricted to be even. The overall bank is constructed with the aid of the prototype filter $H_p(z)$ of order N as given by Equation (51). The transfer functions $H_k(z)=F_k(z)$ for $k=0, 1, \dots, M-1$ in the analysis and synthesis banks of Figure 1(a) are generated by the aid of a DFT modulation of the prototype filter to have the following complex-valued impulse responses:

$$h_k[n] = f_k[n] = \sqrt{2}h_p[n]e^{j2\pi k(n-N/2)/M} \quad \text{for } n=0, \dots, N, \quad (61)$$

where $h_p[n]$ for $n=0, 1, \dots, N$ are the impulse response coefficients for an $M/2$ -channel PR or NPR cosine-modulated filter bank. The frequency responses of the analysis filters of an M -channel MDFT filter bank are shown in Figure 30(b), whereas Figure 30(a) shows that of the prototype filter. The analysis-synthesis filter bank of Figure 1(a) using these filters is not suitable without modifications since it does not provide the desired alias cancellation.

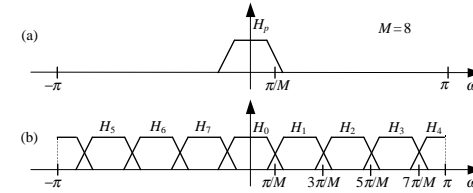


Figure 30. Frequency responses of an eight-channel MDFT bank. (a) Prototype filter. (b) Complex-valued analysis filters.

The most severe aliasing terms can be removed by modifying the original structure in the proper manner as proposed by Fliege and Karp in (Fliege, 1993, Karp, 1999), resulting in the MDFT filter bank. The key idea is to use a two-step decimation and a two-step interpolation for each sub-band signal in the analysis and synthesis parts, respectively, as shown in Figure 31. After forming the analysis filters as described above, the signal is first decimated by a factor of $M/2$ (M is even). The resulting signals are then decimated by a factor of two with and without a unit delay. In the resulting sub-bands, either the real or imaginary part is used. Without loss of generality, it can be assumed that the real (imaginary) part is taken in the upper (undelayed) branch of all even (odd) sub-bands. In the synthesis bank, a similar modification is performed as shown in Figure 31. This results in a critically sampled complex-modulated PR or NPR M -channel filter bank provided that the prototype filter for an $M/2$ -channel cosine-modulated filter bank possesses the same property (Fliege, 1993; Karp and Fliege, 1999). The price to be paid for this modifications is that the filter banks delay increases from N to $N+M/2$. For a complex-valued input sequence $x[n]$, the analysis bank maps this signal into M real and M imaginary sequences at the sampling rate reduced by a factor of M . The advantage of the resulting filter bank for a linear-phase $H_p(z)$ is that all these mappings can be regarded as processes where each sequence is first generated by filtering the input signal by linear-phase complex-coefficient FIR filters $H_k(z)$ and $z^{-M/2}H_k(z)$ for $k=0, 1, \dots, M-1$, depending on whether the unit delay is used or not, before decimating by a factor of M and selecting the real or imaginary part of the output. As will be seen in Subsection 3.3.2, this property leads for a real input data to a filter bank where all the analysis and synthesis filters are linear-phase real-coefficient FIR filters, which is of great importance, for instance, in image processing.

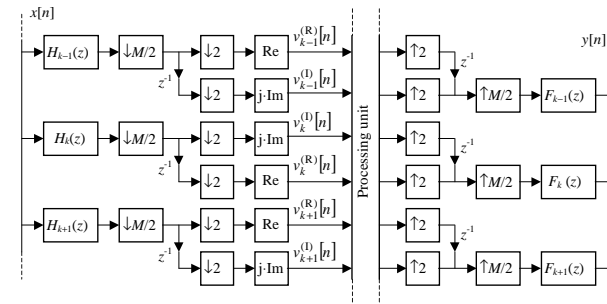


Figure 31. MDFT filter bank.

This subsection concentrates mostly on the case where $N=2LM-1$ with L being an integer since in this case there are no constraints for the prototype filter to have fixed impulse-response values. It should be pointed out that in the most general case, instead of N in Equation (61), other integers can be used (Heller et al., 1999). This subsection considers only the original form of Equation (61) because in this case the real and imaginary parts of the transfer functions $H_k(z)$ and $F_k(z)$ are guaranteed to be linear-phase FIR filters provided that the prototype filter $H_p(z)$ is a linear-phase FIR filter. This is one of the most important properties of the original MDFT filter banks. However, it should be pointed out that in some communications applications it might be beneficial to use low-delay MDFT filter banks. These banks can be generated using the scaled prototype filter for an $M/2$ -channel PR or NPR low-delay biorthogonal cosine-modulated filter bank.

An efficient implementation for the MDFT filter bank without the processing unit is depicted in Figure 32 (Fliege, 1994). In this figure, IDFT stand for the inverse discrete Fourier transform and $W = e^{-j2\pi/M}$. The impulse response coefficients of $G_l(z)$ and $\bar{G}_l(z)$ for $l = 0, 1, \dots, M-1$ are obtained from the prototype filter $H_k(z)$, as given by Equation (51) for the $M/2$ -channel cosine modulated filter bank, as $g_l(m) = \sqrt{2}h_p(m \cdot M + l)$ and $\bar{g}_l(m) = \sqrt{2}h_p(m \cdot M - l)$ for $l = 0, 1, \dots, M-1$ (corresponding to the Type 1 and Type 3 polyphase components). A computationally more efficient realization form has been proposed by Karp and Fliege (1996). The filter delay for the bank of Figure 32 is $N+M/2$.

It should be pointed out that the structure of Figure 32 has been constructed for processing a "real" complex-valued input data. If this signal is formed artificially such that both the real and imaginary parts are formed based on two distinct real-valued signals, then modifications in the structure of Figure 32 are required, as has been discussed by Karp and Fliege (1999).

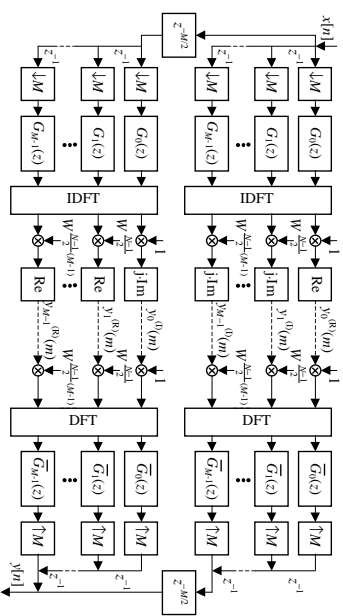


Figure 32. Implementation of MDFT filter bank for a complex-valued input signal.

3.3.2 MDFT filter banks for real-valued input data

For a real input signal in Figure 31, $v_0^{(R)}[n] = 0$ and $v_{M/2}^{(R)}[n] = 0$, $v_0^{(I)}[n] = 0$, $v_{M/2}^{(I)}[n] = 0$, $v_{M-k}^{(R)}[n] = -v_k^{(R)}[n]$, $v_{M-k}^{(I)}[n] = v_k^{(I)}[n]$, and $v_{M-k}^{(I)}[n] = -v_k^{(I)}[n]$ for N odd (even). It can be shown, after some manipulations, that only the analysis and synthesis filters $H_k(z)$ and $F_k(z)$ for $k = 0, 1, \dots, M/2$ are needed provided that the transfer functions for

$k = 1, 2, \dots, M/2-1$ are multiplied by $\sqrt{2}$. For N odd, this corresponds to the filter bank shown in Figure 33, where the impulse responses of $H_k^{(R)}(z)$ and $H_k^{(I)}(z)$ for $k = 1, 2, \dots, M/2-1$ are given in terms of the impulse response $h_p[n]$ for $n = 0, 1, \dots, N$ of the linear-phase prototype filter for the $M/2$ -channel cosine modulated filter bank as follows:

$$h_k^{(R)}[n] = \begin{cases} 2h_p[n] \cos[2\pi k(n - N/2)/M] & \text{for } k \text{ even} \\ 2h_p[n - M/2] \cos[2\pi k(n - N/2 - M/2)/M] & \text{for } k \text{ odd} \end{cases} \quad (62)$$

$$h_k^{(I)}[n] = \begin{cases} 2h_p[n] \sin[2\pi k(n - N/2)/M] & \text{for } k \text{ odd} \\ 2h_p[n - M/2] \sin[2\pi k(n - N/2 - M/2)/M] & \text{for } k \text{ even,} \end{cases} \quad (63)$$

whereas $(H_0^{(I)}(z)$ and $H_{M/2}^{(R)}(z)$ provide no contributions)

$$h_0^{(R)}[n] = \sqrt{2}h_p[n] \quad (64)$$

$$h_{M/2}^{(I)}[n] = \begin{cases} \sqrt{2}h_p[n] \sin[\pi(n - N/2)/M] & \text{for } M/2 \text{ odd} \\ \sqrt{2}h_p[n - M/2] \sin[\pi(n - N/2 - M/2)/M] & \text{for } M/2 \text{ even.} \end{cases} \quad (65)$$

For the corresponding $F_k^{(R)}(z)$ and $F_k^{(I)}(z)$ for $k = 0, 1, \dots, M/2$, the impulse response coefficients are obtained through

$$f_k^{(R)}[n] = h_k^{(R)}[N + M/2 - n] \quad (66)$$

$$f_k^{(I)}[n] = h_k^{(I)}[N + M/2 - n]. \quad (67)$$

In the above, it is assumed that $h_p[n]$ is zero for $n < 0$ and $n > N$. If a prototype filter of an even order N is desired to be used, then instead of $H_{M/2}^{(I)}(z)$, $H_{M/2}^{(R)}(z)$ is used with the following impulse response coefficients:

$$h_{M/2}^{(R)}[n] = \begin{cases} \sqrt{2}h_p[n] \cos[\pi(n - N/2)/M] & \text{for } M/2 \text{ even} \\ \sqrt{2}h_p[n - M/2] \cos[\pi(n - N/2 - M/2)/M] & \text{for } M/2 \text{ odd.} \end{cases} \quad (68)$$

An example of amplitude responses for an eight-channel MDFT filter bank with a prototype filter of odd order is given in Figure 34.

It should be emphasized that Equations (62)–(68) have been derived for the case where Equation (61) with a linear-phase prototype filter of order N is used as a starting point. In this case, all the analysis and synthesis filters are linear-phase FIR filters. Similar equations have been derived by Heller et al. (1999) for the case where, instead of N , $K < N$ is used in Equation (61) and the prototype filter is a nonlinear-phase FIR filter of order N . A slightly different approach for generating filter banks for processing real-valued input signals with linear-phase FIR filters has been proposed by Lin and Vaidyanathan (1995).

When comparing MDFT filter banks and cosine-modulated filter banks the following properties should be emphasized. First, prototype filters for a $2M$ -channel MDFT filter bank and for an M -channel cosine-modulated filter bank are the same. Second, for processing real-valued signals, a $2M$ MDFT filter bank is needed to obtain similar coding gain (Lin and Vaidyanathan, 1995) like for an M -channel cosine-modulated filter bank. In this case, both filter banks have

approximately the same delay and complexity. Third, in an MDFT filter bank analysis and synthesis filters can be linear-phase filters, that is not the case for cosine-modulated filter banks. This makes MDFT filter banks very useful in image processing applications.

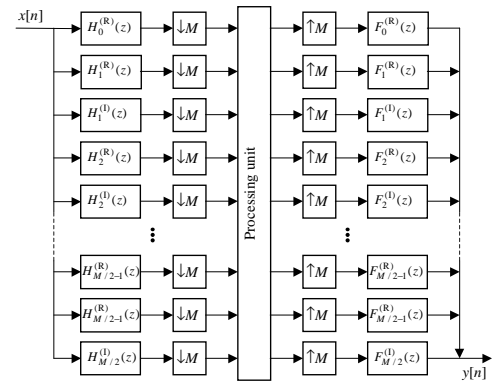


Figure 33. Equivalent filter bank for processing real-valued input data. N is odd.

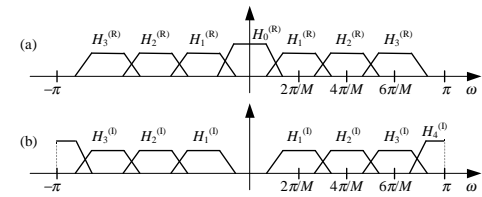


Figure 34. MDFT filter bank for processing real-valued input data. $M = 8$ and N is odd. (a) Analysis filters for real subbands. (b) Analysis filters for imaginary subbands.

As an example Figure 35 shows the amplitude responses of the real and the imaginary channels for the analysis part, for a 64-channel PR MDFT filter bank, when processing real-valued input signals with the analysis and synthesis filters given by Equations (62)–(68). The prototype filter is the same as design 1 in Table III for a 32-channel cosine-modulated filter bank.

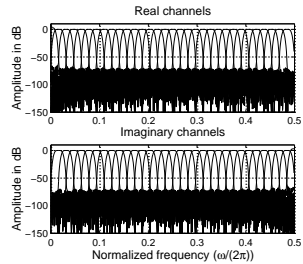


Figure 35. Amplitude responses of the analysis filters for 64-channel PR MDFT filter bank for processing real-valued input signals.

4 Octave Filter Banks

There exist two basic classes of octave filter banks, namely, frequency-selective octave filter banks and discrete-time wavelet banks. This section starts with frequency-selective banks and then connections to discrete-time wavelet banks are briefly discussed.

4.1 Octave Filter Banks Using Two-Channel FIR and IIR Filter Banks as Building Blocks

When generating an octave filter bank, a two-channel filter bank shown in Figure 36(a) is used as a starting point. In this figure, the processing unit is omitted. The first step is to use a two-channel filter bank after the decimated lowpass filtered signal in the original filter bank as shown in Figure 36(b). This bank is exactly the same as the original one, as shown in Figure 36(a). If the transfer function for this bank is $T(z)$, then the decimated highpass filtered signal, denoted by $y_1[r]$ in Figure 36(b), should be filtered by $C_1(z) = T(z)$ in order to make the overall input-output transfer function equal to $T(z)T(z^2)$. If the two-channel filter bank is constructed using causal IIR half-band filters, this transfer function is an allpass filter. For the PR FIR two-channel filter bank with $T(z) = z^{-K}$, the overall delay is $3K$ samples. The second diagram in Figure 36(b) shows an equivalent structure that is useful for the analysis purposes.

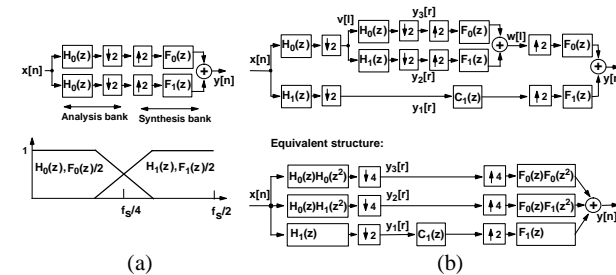


Figure 36. Generating a two-level octave filter bank. (a) Starting-point two-channel filter bank. (b) Two-level octave filter bank and its equivalent structure for the analysis purposes.

In order to generate a multilevel octave bank, the last decimated lowpass filtered signal of Figure 36(b) is treated in the same manner. This process can be repeated several times. The number of steps depends on the application. Figure 37(a) shows the structure for the analysis part in the case where the band splitting has been performed five times. This figure shows also the equivalent structure where the input data is filtered by six filters followed by decimation by different factors. Figure 37(b) shows the corresponding synthesis part. Finally, the overall system is depicted in Figure 38. In Figure 38, additional transfer functions $C_k(z)$ for $k = 1, 2, \dots, 6$ are included in order to make the overall transfer function equal to $T(z)T(z^2)T(z^4)T(z^8)T(z^{16})$. This goal is achieved by $C_1(z) = T(z)T(z^2)T(z^4)T(z^8)$, $C_2(z) = T(z)T(z^2)T(z^4)$, $C_3(z) = T(z)T(z^2)$, $C_4(z) = T(z)$, and $C_5(z) = C_6(z) = 1$. For a PR two-channel FIR filter bank with $T(z) = z^{-K}$, $C_1(z) = z^{-15K}$, $C_2(z) = z^{-7K}$, $C_3(z) = z^{-3K}$, $C_4(z) = z^{-K}$, and the overall delay is $31K$ samples.

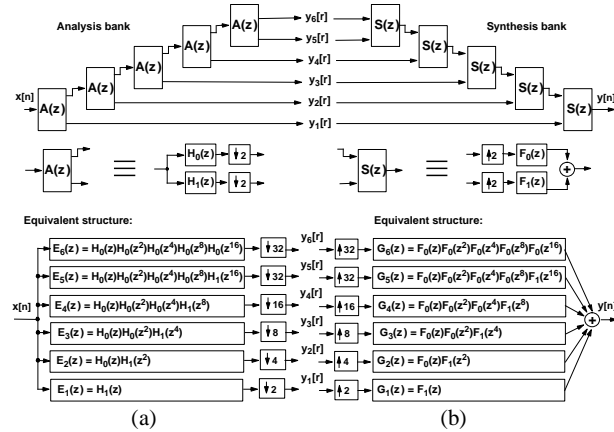


Figure 37. Generation of a five-level octave filter bank. (a) Analysis part. (b) Synthesis part.

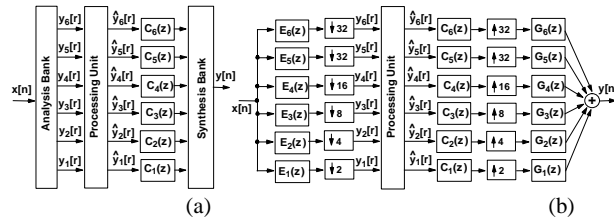


Figure 38. Overall five-level octave bank. (a) Overall implementation. (b) Equivalent structure.

As an example, consider the design of a five-level FIR filter bank built using the minimax orthogonal PR two-channel filter bank with the stopband edge of the lowpass analysis filter being located at 0.586π and the filter orders being 61. Figure 39 shows the amplitude responses for the $E_k(z)$'s (see Figures 37 and 38). The amplitude responses for the $G_k(z)$'s are obtained from those of the $E_k(z)$'s by multiplying the responses by the corresponding interpolation factors.

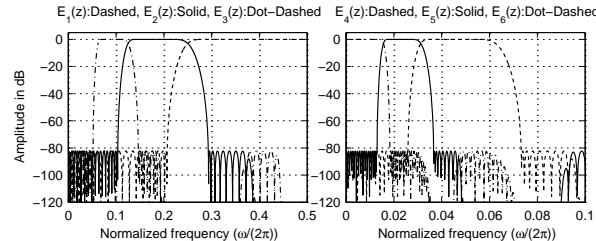


Figure 39. Amplitude responses for the analysis and synthesis filters in an example five-level octave FIR filter bank.

4.2 Generation of Discrete-Time Wavelet Banks from Octave Filter Banks

Discrete-time wavelet banks (Vetterli and Herley, 1992; Vetterli and Kovačević, 1995; Misiti et al., 1996) can be regarded as special cases of octave filter banks considered in the previous subsection. The common feature is that they are both constructed with the aid of a single two-channel PR filter bank. In the previous section, the goal was to design this building block in such a manner that the filters in the overall bank provide a good channel separation together with high enough attenuations. Discrete-time wavelet banks are used in applications where the waveform of the input signal is desired to be preserved when performing modifications to the sub-signals in the processing unit. The applications include, among others, detecting discontinuities and breakdown points of one-dimensional (1-D) signals, detecting long-term evolution of 1-D signals, detecting self-similarities of 1-D signals and images, de-noising and compression of 1-D signals and images, and extracting some special features of 1-D signals and images. The need for nearly preserving the waveforms states completely new criteria for designing the building-block two-channel filter bank for discrete-time wavelet banks. Instead of the frequency-selectivity of the resulting overall bank, there are other measures of "goodness". These include, among others, the orders of the filters in the building-block bank, the number of levels in the octave bank, the phase linearity, the number of vanishing moments, the regularity of the corresponding continuous-time analysis and synthesis wavelets and scaling functions. These topics will be considered in more details in Chapter 3.

5 Concluding Remarks

This chapter gave an overview on how to synthesize critically sampled multirate filter banks. We concentrated on three main topics. First, various two-channel filter banks based on the use of FIR and IIR filters were reviewed. Second, uniform multi-channel (M -channel) filter banks were constructed in two basic ways. The first approach was based on using a tree-structure with two-channel filter banks as building blocks. In the second approach, these banks were generated with the aid of a single prototype filter and a proper cosine-modulation or MDFT technique. As has been mentioned, MDFT banks are more attractive in the case where the goal is to preserve the waveform of the original signal, like in the case of images. This is due to the fact that, despite of having more filters in the bank, all the sub-filters can have linear-phase impulse responses. Third, octave filter banks were constructed using a two-channel filter bank as a building block. Two extreme cases of octave filter banks were considered, namely, frequency-selective banks and discrete-time wavelet banks that concentrate on providing good channel selectivity or on preserving the waveform of the original signal, respectively.

There exist still several open questions regarding to the multirate filter banks considered in this chapter. First, there are various alternatives to construct PR and NPR two-channel filter banks. What is the best selection when these banks are used alone or building a tree-structured or octave filter banks? Second, in the case of multi-channel uniform filter banks when to use the orthogonal cosine-modulated, low-delay cosine-modulated, or MDFT banks? Third, in the case of octave filter banks, are there proper compromises between the frequency-selective banks and discrete-time wavelet banks? The proper selection depends strongly on the application.

Empirical work must still be done in order to find a proper multirate filter banks for a specific application. As mentioned in the introduction, in the case of audio signals, our ears are the final "referees" and in the case of images or video signals, our eyes play the same role. Therefore, in many applications, the ultimate goal is to design the overall system with the minimum complexity and/or the minimum number of bits required for transferring or storing the data in

such a manner that the resulting output signal is still satisfactory to our ears or eyes. It is well known that for our ears in the case of a mono or stereo signal, multirate filter banks with high channel selectivity are preferred. In the case of our eyes and images, it is desired to use multirate filter banks approximately preserving the waveform of the image.

6 References

- E. Abdel-Raheem, F. El-Guibaly, and A. Antoniou (1996, February). Design of low-delay two-channel FIR filter banks using constrained optimization. *Signal Process.*, **48**, 183–192.
- F. Argenti and E. Del Re (2000, March). Design of biorthogonal M -channel cosine-modulated FIR/IIR filter banks. *IEEE Trans. Signal Process.*, **48**, 876–881.
- S. Basu, C.-H. Chiang, and H. M. Choi (1995, January). Wavelets and perfect reconstruction subband coding with causal stable IIR filters. *IEEE Trans. Circuits Syst. II*, **42**, 24–38.
- T. Blu (1998, June). A new design algorithm for two-band orthonormal rational filter banks and orthonormal rational wavelets. *IEEE Trans. Signal Process.*, **46**, 1494–1504.
- R. Bregović and T. Saramäki (1999, March). Two-channel FIR filter banks - A tutorial review and new results. *Proc. Second Int. Workshop on Transforms and Filter Banks, Brandenburg, Germany, TICSP #4*, 507–558.
- R. Bregović and T. Saramäki (2000a, June). An iterative method for designing orthogonal two-channel FIR filter banks with regularities. *Proc. IEEE Int. Conf. Acoust., Speech, Signal Process., Istanbul, Turkey, I*, 484–487.
- R. Bregović and T. Saramäki (2000b, September). A general-purpose optimization technique for designing two-channel FIR filter banks. *Proc. Tenth European Signal Process. Conf., Tampere, Finland, I*, 369–372.
- R. Bregović and T. Saramäki (2001a, May). A systematic technique for designing prototype filters for perfect reconstruction cosine modulated and modified DFT filter banks. *Proc. IEEE Int. Symp. Circuits Syst., Sydney, Australia, 2*, 33–36.
- R. Bregović and T. Saramäki (2001b, June). Design of causal stable perfect reconstruction two-channel IIR filter banks. *Proc. Second Int. Symp. on Image and Signal Processing and Analysis, Pula, Croatia*, 545–550.
- R. Bregović and T. Saramäki (2001c, September). An efficient approach for designing nearly perfect-reconstruction low-delay cosine-modulated filter banks. *Proceedings of the Third Conference on Computer Science and Information Technologies, Yerevan, Armenia*, 283–288.
- S. C. Chan, J. S. Mao, and K. L. Ho (2000, August). A new design method for two-channel perfect reconstruction IIR filter banks. *IEEE Signal Process. Letters*, **7**, 221–223.
- C.-K. Chen and J.-H. Lee (1992, September). Design of quadrature mirror filters with linear phase in the frequency domain. *IEEE Trans. Circuits Syst. II*, **39**, 593–605.
- C. D. Creuser and S. Mitra (1995, April). A simple method for designing high-quality prototype filters for M -band pseudo QMF banks. *IEEE Trans. Signal Process.*, **43**, 1005–1007.
- R. E. Crochiere and L. R. Rabiner (1983). *Multirate Digital Signal Processing*. Englewood Cliffs, NJ: Prentice-Hall.
- I. Daubechies and W. Sweldens (1998). Factoring wavelet transforms into lifting steps. *Journal Fourier Anal. Appl.*, **4**(3), 245–267.

- S. R. K. Dutta and M. Vidyasagar (1977). New algorithms for constrained minimax optimization. *Mathematical Programming*, **13**, 140–155.
- D. Esteban and C. Galand (1977, May). Application of quadrature mirror filters to split band voice coding schemes. *Proc. IEEE Int. Conf. Acoust., Speech, Signal Process., Hartford, CT*, 191–195.
- N. J. Fliege (1993, Nov.). Computational efficiency of modified DFT-polyphase filter banks. *Proc. 27th Asilomar Conf. Signals, Systems, Computers, Pacific Grove, California, 2*, 1296–1300.
- N. J. Fliege (1994). *Multirate Digital Signal Processing*. Chicester, NY: John Wiley and Sons.
- L. Gazsi (1985, January). Explicit formulas for lattice wave digital filters. *IEEE Trans. Circuits Syst., CAS-32*, 68–88.
- C.K. Goh, Y. C. Lim, and C. S. Ng (1999a, July). Improved weighted least squares algorithm for the design of quadrature mirror filters. *IEEE Trans. Signal Process.*, **47**, 1866–1877.
- C.-K. Goh and Y. C. Lim (1999b, December). An efficient algorithm to design weighted minimax perfect reconstruction quadrature mirror filter banks. *IEEE Trans. Signal Process.*, **47**, 3303–3314.
- P. N. Heller, T. Karp, and T. Q. Nguyen (1999, April). A general formulation of modulated filter banks. *IEEE Trans. Signal Process.*, **47**, 986–1002.
- O. Herrmann and W. Schüssler (1970, May). Design of nonrecursive digital filters with minimum phase. *IEE Elec. Letters*, **6**, 329–330.
- O. Herrmann (1971, May). On the approximation problem in nonrecursive digital filter design. *IEEE Trans. Circuit Theory, CT-18*, 411–413.
- B.-R. Horng and A. N. Willson (1992, February). Lagrange multiplier approaches to the design of two-channel perfect-reconstruction linear-phase FIR filter banks. *IEEE Trans. Signal Process.*, **40**, 364–374.
- J. D. Johnston (1980, April). A filter family designed for use in quadrature mirror filter banks. *Proc. IEEE Int. Conf. Acoust., Speech, Signal Process., Denver, Colorado, 1*, 291–294.
- T. Karp and N. J. Fliege (1996, September). Computationally efficient realization of MDFT filter banks. *Proc. Eighth European Signal Process. Conf., Trieste, Italy, II*, 1183–1186.
- T. Karp and A. Mertins (1997, July). Lifting schemes for biorthogonal modulated filter banks. *Proc. Digital Signal Process., Santorini, Greece, 1*, 443–446.
- T. Karp and N. J. Fliege (1999, November). Modified DFT filter banks with perfect reconstruction. *IEEE Trans. Circuits Syst. II*, **46**, 1404–1414.
- T. Karp, A. Mertins, and G. Schuller (2001, May). Efficient biorthogonal cosine-modulated filter banks. *Signal Process.*, **81**, 997–1016.
- C. W. Kim and R. Ansari (1991, May). FIR/IIR exact reconstruction filter banks with applications to subband coding of images. *Proc. 34th Midwest Symp. Circuits and Syst., Monterey, California, 1*, 227–230.
- R. D. Koilpillai and P. P. Vaidyanathan (1991, April). New results on cosine-modulated filter banks satisfying perfect reconstruction. *Proc. IEEE Int. Conf. Acoust., Speech, Signal Process., Toronto, Canada, 3*, 1793–1796.
- R. D. Koilpillai and P. P. Vaidyanathan (1992, April). Cosine-modulated FIR filter banks satisfying perfect reconstruction. *IEEE Trans. Signal Process.*, **40**, 770–783.
- Y. C. Lim, R. H. Yang, and S.-N. Koh (1993, May). The design of weighted minimax quadrature mirror filters. *IEEE Trans. Signal Process.*, **41**, 1780–1789.

Y.-P. Lin and P. P. Vaidyanathan (1995, November). Linear phase cosine modulated maximally decimated filter banks with perfect reconstruction. *IEEE Trans. Signal Process.*, 42, 2525–2539.

W.-S. Lu, H. Xu, and A. Antoniou (1998, July). A new method for the design of FIR quadrature mirror-image Filter Banks. *IEEE Trans. Circuits Syst. II*, 45, 922–926.

H. S. Malvar (1990, June). Modulated QMF filter banks with perfect reconstruction. *IEE Elec. Letters*, 26, 906–907.

H. S. Malvar (1991, April). Extended lapped transforms: Fast algorithms and applications. *Proc. IEEE Int. Conf. Acoust., Speech, Signal Process., Toronto, Canada*, 3, 1797–1800.

H. S. Malvar (1992a). *Signal Processing with Lapped Transforms*. Norwood, MA: Artec House.

H. S. Malvar (1992b, November). Extended lapped transforms: Properties, applications, and fast algorithms. *IEEE Trans. Signal Process.*, 40, 2703–2714.

J. S. Mao, S. C. Chan, and K. L. Ho (1999, June). Theory and design of causal stable IIR PR cosine-modulated filter banks. *Proc. IEEE Int. Symp. Circuits Syst., Orlando, Florida, III*, 427–430.

J. S. Mao, S. C. Chan, and K. L. Ho (2000, May). Design of two-channel PR FIR filter banks with low system delay. *Proc. IEEE Int. Symp. Circuits Syst.*, Geneva, Switzerland, I, 627–630.

J. H. McClellan, T. W. Parks, and L. R. Rabiner (1973, December). A computer program for designing optimum FIR linear phase digital filters. *IEEE Trans. Audio Electroacoustics*, AU-21, 506–526.

A. Mertins (1998, October) Subspace approach for the design of cosine-modulated filter banks with linear-phase prototype filter. *IEEE Trans. Signal Process.*, 46, 2812–2818.

F. Mintzer (1985, June) Filters for distortion-free two-band multirate filter banks. *IEEE Trans. Acoust., Speech, Signal Process.*, ASSP-33, 626–630.

M. Misiti, Y. Misiti, G. Oppenheim and J. M. Poggio (1996, March). *Wavelet toolbox User's Guide*. Natick, MA: The MathWorks, Inc.

S. K. Mitra, C. D. Creusere, and H. Babić (1992, May). A novel implementation of perfect reconstruction QMF banks using IIR filters for infinite length signals. *Proc. IEEE Int. Symp. Circuits Syst., San Diego, California*, 5, 2312–2315.

K. Nayebi, T. P. Barnwell III, and M. J. T. Smith (1992, June). Time-domain filter bank analysis: A new design theory. *IEEE Trans. Signal Process.*, 40, 1412–1429.

K. Nayebi, T. P. Barnwell III, and M. J. T. Smith (1994, January). Low delay FIR filter banks: Design and evaluation. *IEEE Trans. Signal Process.*, 42, 24–31.

T. Q. Nguyen and P. P. Vaidyanathan (1989, May). Two-channel perfect-reconstruction FIR QMF structures which yield linear-phase analysis and synthesis filters. *IEEE Trans. Acoust., Speech, Signal Process.*, ASSP-37, 676–690.

T. Q. Nguyen (1992a, May). A class of generalized cosine-modulated filter bank. *Proc. IEEE Int. Symp. Circuits Syst., San Diego, CA*, 2, 943–946.

T. Q. Nguyen (1992b, May). A quadratic constrained least-squares approach to the design of digital filter banks. *Proc. IEEE Int. Symp. Circuits Syst., San Diego, CA*, 3, 1344–1347.

T. Q. Nguyen (1994, January). Near-perfect-reconstruction pseudo-QMF banks. *IEEE Trans. Signal Process.*, 42, 65–76.

T. Q. Nguyen (1995, September). Digital filter bank design quadratic-constrained formulation. *IEEE Trans. Signal Process.*, 43, 2103–2108.

T. Q. Nguyen and R. D. Koilpillai (1996, March). The theory and design of arbitrary-length cosine-modulated filter banks and wavelets, satisfying perfect reconstruction. *IEEE Trans. Signal Process.*, 44, 473–483.

S.-M. Phoong, C. W. Kim, and P. P. Vaidyanathan (1995, March). A new class of two-channel biorthogonal filter banks and wavelet bases. *IEEE Trans. Signal Process.*, 43, 649–665.

T. A. Ramstad (1988, June). IIR filter bank for subband coding of images. *Proc. IEEE Int. Symp. Circuits Syst., Espoo, Finland*, 1, 827–830.

T. A. Ramstad and J. P. Tanem (1991, April). Cosine-modulated analysis-synthesis filter bank with critical sampling and perfect reconstruction. *Proc. IEEE Int. Conf. Acoust., Speech, Signal Process., Toronto, Canada*, 3, 1789–1792.

M. Renfors and T. Saramäki (1987, January). Recursive N -th band digital filters – Part I: Design and properties. *IEEE Trans. Circuits Syst.*, 34, 24–39.

J. H. Rothweiler (1983, April). Polyphase quadrature filter – A new subband coding technique. *Proc. IEEE Int. Conf. Acoust., Speech, Signal Process., Boston, Massachusetts*, 3, 1280–1283.

T. Saramäki (1992, May). Designing prototype filters for perfect-reconstruction cosine-modulated filter banks. *Proc. IEEE Int. Symp. Circuits Syst., San Diego, CA*, 3, 1605–1608.

T. Saramäki (1993). Finite impulse response filter design, Chapter 4. *Handbook for Digital Signal Processing* edited by S. K. Mitra and J. F. Kaiser. New York: John Wiley & Sons.

T. Saramäki (1998, February). A generalized class of cosine-modulated filter banks. *Proc. First Int. Workshop on Transforms and Filter Banks, Tampere, Finland, TICSP #1*, 336–365.

T. Saramäki and R. Bregović (2001, May). An efficient approach for designing nearly perfect-reconstruction cosine-modulated and modified DFT filter banks. *Proc. IEEE Int. Conf. Acoust., Speech, Signal Process., Salt Lake City, UT*, 6, 3617–3620.

G. Schuller and M. J. T. Smith (1995, May). A new algorithm for efficient low delay filter bank design. *Proc. IEEE Int. Conf. Acoust., Speech, Signal Process., Michigan, Detroit, II*, 1472–1475.

G. D. T. Schuller and M. J. T. Smith (1996, August). New framework for modulated perfect reconstruction filter banks. *IEEE Trans. Signal Process.*, 44, 1941–1954.

G. Schuller (1997, May). Time varying filter banks with variable system delay. *Proc. IEEE Int. Conf. Acoust., Speech, Signal Process., Munich, Germany*, 3, 2469–2472.

G. D. T. Schuller and T. Karp (2000, March). Modulated filter banks with arbitrary system delay: Efficient implementations and the time-varying case. *IEEE Trans. Signal Process.*, 48, 737–748.

M. J. T. Smith and T. P. Barnwell III (1986, June). Exact reconstruction techniques for tree-structured subband coders. *IEEE Trans. Acoust., Speech, Signal Process.*, ASSP-34, 434–441.

W. Sweldens (1996). The lifting scheme: A custom-design construction of biorthogonal wavelets. *Applied Computational Harmonic Analysis*, 3(2), 186–200.

D. B. H. Tay (1998, August). Design of causal stable IIR perfect reconstruction filter banks using transformation of variables. *IEE Proc. Vis. Image Signal Process.*, 145, 287–292.

T. Uto, M. Okuda, M. Ikehara, and S.-I. Takahashi (1999, October). Image coding using wavelets based on two-channel linear phase orthogonal IIR filter banks. *Proc. IEEE Int. Conf. Image Process., Kobe, Japan*, 2, 265–268.

P. P. Vaidyanathan and P. Q. Hoang (1988, January). Lattice structures for optimal design and robust implementation of two-channel perfect-reconstruction QMF banks. *IEEE Trans. Acoust., Speech, Signal Process., ASSP-36*, 81–94.

P. P. Vaidyanathan, T. Q. Nguyen, Z. Doganata, and T. Saramäki (1989, July). Improved technique for design of perfect reconstruction FIR QMF banks with lossless polyphase matrices. *IEEE Trans. Acoust., Speech, Signal Process., ASSP-37*, 1042–1056.

P. P. Vaidyanathan (1993). *Multirate Systems and Filter Banks*. Englewood Cliffs, N.J.: Prentice Hall.

M. Vetterli and C. Herley (1992, September). Wavelets and filter banks: Theory and design. *IEEE Trans. Signal Process., 40*, 2207–2232.

M. Vetterli and J. Kovačević, (1995). *Wavelets and Subband Coding*. Englewood Cliffs, N.J.: Prentice Hall.

W. Wegener (1979, June). Wave digital directional filters with reduced number of multipliers and adders. *Arch. Elek. Übertragung, 33*, 239–243.

H. Xu, W.-S. Lu, and A. Antoniou (1996, July). Efficient Iterative design method for cosine-modulated QMF banks. *IEEE Trans. Signal Process., 44*, 1657–1668.

H. Xu, W.-S. Lu, and A. Antoniou (1998, May). An improved method for the design of FIR quadrature mirror-image filter banks. *IEEE Trans. Signal Process., 46*, 1275–1281.

S.-J. Yang, J.-H. Lee, and B.-C. Chieu (1998, December). Perfect-reconstruction filter banks having linear-phase FIR filters with equiripple response. *IEEE Trans. Signal Process., 46*, 3246–3255.

X. Zhang and H. Iwakura (1995, February). Design of QMF banks using allpass filters. *IEE Elec. Letters, 31*, 172–174.

X. Zhang and T. Yoshikawa (1998, May). Design of causal IIR perfect reconstruction filter banks. *Proc. IEEE Int. Conf. Acoust., Speech, Signal Process., Seattle, Washington, 3*, 1429–1432.

X. Zhang and T. Yoshikawa (1999, February). Design of two-channel IIR linear phase PR filter banks. *Signal Process., 72*, 167–175.

1	INTRODUCTION	1
2	TWO-CHANNEL FILTER BANKS	4
2.1	BASIC OPERATION OF A TWO-CHANNEL FILTER BANK	4
2.1.1	Operation of the analysis bank	4
2.1.2	Operation of the processing unit	5
2.1.3	Operation of the synthesis bank	6
2.2	ALIAS-FREE FILTER BANKS	7
2.3	PERFECT-RECONSTRUCTION (PR) AND NEARLY PERFECT-RECONSTRUCTION (NPR) FILTER BANKS	8
2.3.1	Theorem for the PR Property	8
2.3.2	PR Filter Bank Design and the Theorem for the PR Reconstruction	9
2.4	FIR FILTER BANKS AND THEIR DESIGN	11
2.4.1	FIR Filter Bank Classification	12
2.4.2	General FIR Filter Bank Design Problem	12
2.4.3	NPR Quadrature Mirror Filter (QMF) Banks	13
2.4.3.1	QMF banks with linear-phase subfilters	14
2.4.3.2	Low-delay QMF banks with nonlinear-phase subfilters	15
2.4.4	PR Orthogonal Filter Banks	15
2.4.5	PR Biorthogonal Filter Banks	16
2.4.5.1	PR biorthogonal filter banks with linear-phase subfilters	16
2.4.5.2	Low-delay PR biorthogonal filter banks with nonlinear-phase subfilters	17
2.4.6	Generalized NPR Filter Banks	18
2.4.6.1	NPR filter banks with linear-phase subfilters	18
2.4.6.2	Low-delay NPR filter banks with nonlinear-phase subfilters	18
2.4.7	FIR filter bank examples	19
2.5	IIR FILTER BANKS AND THEIR DESIGN	21
2.5.1	IIR Filter Banks With Phase Distortion Generated by Using Half-Band IIR Filters	21
2.5.2	PR IIR Filter Banks Using Causal and Anti-Causal Half-Band Filters	23
2.5.3	PR IIR Filter Banks Using Special IIR Filters	23
2.5.4	PR IIR Filter Banks Based on a Special Structure	24
3	MULTI-CHANNEL (M-CHANNEL) FILTER BANKS	25
3.1	TREE-STRUCTURED FILTER BANKS USING TWO-CHANNEL FILTER BANKS AS BUILDING BLOCKS	25
3.2	COSINE-MODULATED FILTER BANKS	28
3.2.1	Input-output relations for M-channel critically sampled filter banks	28
3.2.2	PR and NPR cosine-modulated filter banks	29
3.2.3	PR cosine-modulated filter banks and their implementation	30
3.2.4	Orthogonal and biorthogonal cosine-modulated filter banks under consideration	32
3.2.5	Statement of the optimization problem for PR and NPR cosine-modulated filter banks	33
3.2.6	Design of PR and NPR orthogonal and biorthogonal cosine-modulated filter banks	33
3.2.7	Comparison between PR and NPR cosine-modulated filter banks	34
3.3	MODIFIED DFT FILTER BANKS	37
3.3.1	MDFT filter banks for complex-valued input data	37
3.3.2	MDFT filter banks for real-valued input data	39
4	OCTAVE FILTER BANKS	42
4.1	OCTAVE FILTER BANKS USING TWO-CHANNEL FIR AND IIR FILTER BANKS AS BUILDING BLOCKS	42
4.2	GENERATION OF DISCRETE-TIME WAVELET BANKS FROM OCTAVE FILTER BANKS	44
5	CONCLUDING REMARKS	44
6	REFERENCES	45